

AMERICAN UNIVERSITY OF BEIRUT

MODELING STRENGTH, STIFFNESS AND DUCTILITY OF  
EXTENDED ENDPLATE CONNECTIONS WITH CIRCULAR  
AND RECTANGULAR BOLT CONFIGURATIONS

by  
ELIE NABHAN MOUANNES

A thesis  
submitted in partial fulfillment of the requirements  
for the degree of Master of Engineering  
to the Department of Civil and Environmental Engineering  
of the Faculty of Engineering and Architecture  
at the American University of Beirut

Beirut, Lebanon  
July 2015

AMERICAN UNIVERSITY OF BEIRUT

MODELING STRENGTH, STIFFNESS AND DUCTILITY OF  
EXTENDED ENDPLATE CONNECTIONS WITH CIRCULAR  
AND RECTANGULAR BOLT CONFIGURATIONS

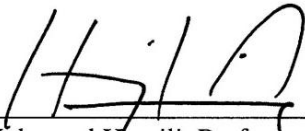
by  
ELIE NABHAN MOUANNES

Approved by:



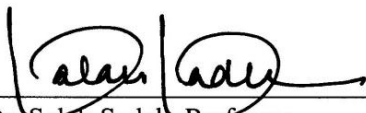
Dr. Elie Hantouche, Assistant Professor  
Department of Civil and Environmental Engineering

Advisor



Dr. Mohamed Harajli, Professor  
Department of Civil and Environmental Engineering

Member of Committee



Dr. Sarah Sadek, Professor  
Department of Civil and Environmental Engineering

Member of Committee

Date of thesis defense: July 29, 2015


AMERICAN UNIVERSITY OF BEIRUT  
THESIS, DISSERTATION, PROJECT RELEASE FORM

Student Name: MOUANNES ELZE NABHAN  
Last First Middle

Master's Thesis       Master's Project       Doctoral Dissertation

I authorize the American University of Beirut to: (a) reproduce hard or electronic copies of my thesis, dissertation, or project; (b) include such copies in the archives and digital repositories of the University; and (c) make freely available such copies to third parties for research or educational purposes.

I authorize the American University of Beirut, **three years after the date of submitting my thesis, dissertation, or project**, to: (a) reproduce hard or electronic copies of it; (b) include such copies in the archives and digital repositories of the University; and (c) make freely available such copies to third parties for research or educational purposes.

Signature  Date 8/4/2015

## ACKNOWLEDGMENTS

First and foremost, I would like to acknowledge and thank my advisor, Dr. Elie Hantouche. His expertise, dedication and enthusiasm were essential in the successful development of this research work. I appreciate his constant support and valuable critics which helped me develop my research skills, and knowledge throughout the years spent at the American University of Beirut.

My recognition and gratitude are addressed to my committee Dr. Mohamed Harajli and Dr. Salah Sadek.

Furthermore, I would like to gratefully acknowledge the financial support provided by the American University of Beirut Research Board under grant No.21113-102726, and by the Lebanese National Council for Scientific Research (LNCSR) under grant No. 102622-21372.

Finally, I would like to express gratitude to my family and friends for their support in the pursuit of my degree. The names include but are not limited to Nabhan, Carmen, Diana and Marc Mouannes.

# AN ABSTRACT OF THE THESIS OF

Elie Nabhan Mouannes for Master of Engineering  
Major: Civil and Environmental Engineering

Title: Modeling Strength, Stiffness and Ductility of Extended Endplate Connections with Circular and Rectangular Bolt Configurations

The results of a series of finite element (FE) simulations and experimental studies are used to develop strength and stiffness models that predict the failure strength and response characteristics of extended unstiffened endplate connections with circular and rectangular bolt configurations associated with deep girders.

The proposed models are composed of multi-linear springs which model the overall extended endplate/column flange system deformation and strength of key components. Comparison of model predictions with FE and experimental results available in the literature show that the proposed models accurately predict the strength and the response of extended endplate/column system with circular and rectangular bolt configurations. The effect of the bolt configuration (circular and rectangular) on the prying phenomenon encountered in the extended unstiffened endplate/column system was investigated.

Based on FE results, extended endplate with circular bolt configuration has a more ductile behavior and exhibits higher total prying forces. The proposed models can be used to design connections that cover all possible failure modes for extended endplate with circular bolt configuration.

# CONTENTS

ACKNOWLEDGEMENTS .....	v
ABSTRACT.....	vi
ILLUSTRATIONS.....	x
TABLES.....	xii
LIST OF ABBREVIATIONS.....	xiii

## Chapter

I. INTRODUCTION.....	1
II. PRELIMINARY DESIGN OF EXTENDED ENDPLATE CONNECTION WITH CIRCULAR AND RECTANGULAR BOLT CONFIGURATIONS.....	5
A. Connection Design.....	5
B. Selected Cases for Analysis.....	8
III. THREE DIMENSIONAL SOLID EXTENDED ENDPLATE MODEL.....	10
A. Mesh Design .....	10
B. Material Properties.....	11
C. Boundary Conditions and Loading.....	11
D. Validation with Experimental Results.....	13

<b>IV. INVESTIGATION OF PRIMARY AND SECONDARY PRYING.....</b>	<b>15</b>
A. Data Analysis.....	15
B. Prying Phenomenon.....	16
C. Bolt Force Variation.....	17
<b>V. STRENGTH MODELS .....</b>	<b>20</b>
A. Strength Models for Circular Bolts Arrangement.....	20
1. Extended Endplate with Circular Bolt Arrangements.....	20
2. Column Flange with Circular Bolt Configuration.....	22
B. Strength Models for Rectangular Bolt Configuration.....	25
1. Extended Endplate with Rectangular Bolt Configuration.....	25
2. Column Flange with Rectangular Bolt Configuration.....	27
<b>VI. COLUMN FLANGE STRENGTH PREDICTION USING YIELD-LINE ANALYSIS.....</b>	<b>28</b>
A. Circular Bolt Configuration.....	29
B. Rectangular Bolt Configuration.....	30
<b>VII. STIFFNESS MODELING.....</b>	<b>32</b>
A. Bolt Stiffness Model.....	32
B. Extended Endplate/Column System with Circular Bolt Configuration.....	33
1. Extended Endplate with Circular Bolt Configuration.....	33
2. Column Flange with Circular Bolt Configuration.....	40
C. Extended Endplate/Column System with Rectangular Bolt Configuration.....	41
1. Extended Endplate with Rectangular Bolt Configuration.....	41
2. Column Flange with Rectangular Bolt Configuration.....	46

VIII. TOTAL ASSEMBLY.....	48
IX. SUMMARY AND CONCLUSIONS.....	50
BIBLIOGRAPHY.....	51



## ILLUSTRATIONS

Figure	Page
1. (a) Extended endplate Connection (b) Extended endplate with rectangular bolt configuration, (c) Extended endplate with circular bolt configuration.....	6
2. Three-dimensional model of endplate connection with rectangular bolt configuration.....	12
3. (a) Extended endplate with rectangular bolt configuration moment-rotation curves (Sumner et al. (2013)) and (b) extended endplate with circular bolt configuration moment-rotation curves (Schweizer (2013)).....	14
4. Bolt force history for extended endplate with rectangular and circular bolt configurations.....	19
5. (a) End plate with circular bolt or column flange with circular and rectangular bolt configurations geometry, (b) endplate with rectangular bolt configuration geometry.....	24
6. Deformation of the extended endplate with rectangular bolt configuration.....	26
7. Yield line mechanism for column flange with (a) circular bolt configuration (b) rectangular bolt configuration.....	31
8. (a) Decision tree for extended endplate with circular bolt configuration and (b) Decision tree for extended endplate with rectangular bolt configuration.....	34
9. Comparison of the FE results with the proposed extended endplate with circular bolt configuration stiffness model associated with (a) W30x108 and (b) W24x76 beams .....	39
10. Column flange stiffness model having circular bolt configuration associated with W30x108 beam connected to a W14x159 column ( $t_{cf}=3.2$ cm).....	41
11. Comparison of the FE results with the proposed extended endplate with rectangular bolt configuration stiffness model associated with (a) W 30x108 beam and (b) W24x76 beam.....	46

12.	Comparison of the FE results with the proposed column flange with rectangular bolt configuration stiffness model associated with W30x108 beam having: (a) $t_{cf}= 1.9$ cm, (b) $t_{cf}=2.2$ cm and (c) $t_{cf}=2.5$ cm.....	47
13.	(a) Total extended endplate connection with circular bolt configuration deformation associated with W24x76 beam including column flange deformation,(b) Total endplate connection with rectangular bolt configuration deformation associated with W30x108 beam including column flange deformation.....	49

## TABLES

Table		Page
1.	Test matrix.....	9
2.	Percentage of primary and secondary prying W24x76 and W30x108 beams.....	16

## LIST OF ABBREVIATIONS

A: cross sectional area

a: length of the plate measured from the inside edge of the interior bolt to the location of occurrence of the plastic hinge at the K-zone

$A_b$ : nominal area of the bolt shank

B: bolt force

b: gage distance between the tension bolts

$b_{cf}$ : column flange width

$B_{fracture}$ : bolt force at fracture

$B_n$ : bolt nominal tensile strength

$b_p$ : endplate width

c: length measured from the inside edge of the exterior bolt line to the outside edge of the endplate

d: beam depth

$d_b$ : bolt diameter

$d_c$ : endplate extension beyond the exterior bolt centerline

$d_h$ : bolt hole diameter

e: minimum edge distance

E: Young's modulus

f: stiffness correlation factor

$f_s$ : shape factor

$F_u$ : ultimate load at failure

$F_y$ : yield stress

$F_{yc}$ : Column yield stress

g: bolt gage

$g_1$ : bolt gage

$g_2$ : bolt gage

$G$ : shear modulus of elasticity

$h_i$ : distance from the center of the bottom flange to the centerline of the upper bolts

$I$ : moment of inertia

$K$ : stiffness of the endplate

$K_{b,k}$ : bolt stiffness at the  $k^{\text{th}}$  step

$K_b$ : elastic bolt stiffness

$K_{b1,k}$ : stiffness of the interior bolt in the  $k^{\text{th}}$  step

$K_{b2,k}$ : stiffness of the exterior bolt in the  $k^{\text{th}}$  step

$K_{ee,k}$ : stiffness of the endplate that is totally elastic with the bolt in its  $k^{\text{th}}$  state

$K_{eee,kk}$ : stiffness of the endplate when it is in the elastic range, and the upper bolts are in their  $k^{\text{th}}$  stiffness range

$K_{h1}, K_{h2}$ : rotational spring with constants

$K_{pe,k}$ : stiffness of the endplate when the plastic hinge has formed at the K-zone and the bolt line is still in its elastic range

$K_{pee,kk}$ : stiffness of the endplate when plastification occurred at the K-zone and the upper bolts are in their  $k^{\text{th}}$  stiffness state

$K_{pp,k}$ : stiffness of the endplate when the bolt line and the K-zone are in their plastic state and full plastification occurs in the endplate

$l$ : distance between bolts centerlines

$L_s$ : free shank length of the bolt

$m$ : length of the column flange/endplate measured from the inside edge of the bolt to the location of occurrence of the plastic hinge at the K-zone

$M_B$ : moment at point B

$M_f$ : moment at the face of the column

$M_{k\text{-zone}}$ : moment at K-zone

$M_p$ : plastic moment

$n$ : length measured from the inside edge of the bolt line to the outside edge of the column flange/endplate where contact occurs

$n_b$ : number of tension bolts

$p$ : tributary width of a pair of tension bolts

$p_b$ : distance from bolt centerline to bolt centerline

$p_{fi}$ : distance from the first interior bolt centerline to the inner face of the beam tension flange

$p_{fo}$ : distance from the outer bolt centerline to the outer face of the beam tension flange

$Q$ : prying force

$Q_P$ : Primary prying force

$Q_S$ : Secondary prying force

$Q_T$ : Total prying force

$r$ : radius of concentric bolts pattern

$s$ : distance from the innermost bolt centerline to the innermost yield line

$T$ : applied tension load

$T'$ : bolt tensile force

$t_{cf}$ : column flange stiffness

$t_p$ : endplate thickness

$W_c$ : vertical column length

$W_e$ : external work

$W_i$ : internal work

$\beta_a$ : constant used in the calculation of the extended endplate stiffness

$\beta_b$ : constant used in the calculation of the extended endplate stiffness

$\gamma$ : factor that accounts for bending of tension bolts

$\gamma_1$ : constant used in the calculation of the endplate stiffness

$\gamma_2$ : constant used in the calculation of the endplate stiffness

$\gamma_3$ : constant used in the calculation of the endplate stiffness

$\gamma_4$ : constant used in the calculation of the endplate stiffness

$\gamma_5$ : constant used in the calculation of the endplate stiffness

$\gamma_6$ : constant used in the calculation of the endplate stiffness

$\gamma_7$ : constant used in the calculation of the endplate stiffness

$\gamma_8$ : constant used in the calculation of the endplate stiffness

$\gamma_9$ : constant used in the calculation of the endplate stiffness

$\gamma_{10}$ : constant used in the calculation of the endplate stiffness

$\gamma_{11}$ : constant used in the calculation of the endplate stiffness

$\gamma_{12}$ : constant used in the calculation of the endplate stiffness

$\gamma_{13}$ : constant used in the calculation of the endplate stiffness

$\gamma_{14}$ : constant used in the calculation of the endplate stiffness

$\gamma_{15}$ : constant used in the calculation of the endplate stiffness

$\gamma_{16}$ : constant used in the calculation of the endplate stiffness

$\gamma_{ee,k}$ : constant used in the calculation of  $K_{ee,k}$

$\gamma_{ep,k}$ : constant used in the calculation of  $K_{ee,k}$

$\Delta$ : displacement

$\delta$ : ratio of the net area at the center of the bolt line to the area of the beam flange

$\Delta B_{ext}$ : change in the exterior bolt force

$\Delta B_{int}$ : change in the interior bolts force

$\Delta M_{K-zone}$ : change in the moment at the K-zone

$\delta Q$ : incremental prying force

$\Delta Q$ : prying gradient

$\Delta T$ : change in the applied load

$\delta T$ : incremental load

$\delta \Delta$ : incremental displacement

$\nu$ : Poisson's ratio

$\Omega_2$ : constant used in the calculation of the extended endplate stiffness

$\Omega_3$ : constant used in the calculation of the extended endplate stiffness

$\Omega_4$ : constant used in the calculation of the extended endplate stiffness

$\Omega_1$ : constant used in the calculation of the extended endplate stiffness

$\xi$ : reduction factor to account for beam web stiffening effect



# CHAPTER I

## INTRODUCTION

Earthquake resistant structures are designed to withstand ductile failure, where the systems are able to achieve large inelastic deformations without significant strength degradation or development of failure mechanisms. Steel moment frames have been historically selected as the preferred lateral resisting structural system for multistory structures in high seismic regions. The steel moment frame connections designed prior to 1994 connected the beams to columns using complete joint penetration (CJP) field welds on the beam flanges to column flange. The research generated by the Northridge earthquake after 1994 sought to improve the inelastic deformation capability of the moment frame connections advising the use of moment bolted connections in high seismic areas. As a result, extended endplate connections (Figure 1 (a)) have become the choice of many structural engineers in designing connections for moment resisting frames in high seismicity areas.

The extended end-plate connections, as shown in Figure 1 (a) consist of beams that are directly welded to an extended end-plate, and the endplate/beam system is then bolted directly through the column flange (ANSI/AISC 358-10). Extended end-plates connections are considered as prequalified special moment frame connections since they are able to achieve high interstory drift rotations associated with ductile failure modes (ANSI/AISC 358-10).

Currently, three different extended endplate connection types are presented in the AISC 358-10: the Four Bolt Unstiffened, Four Bolt Stiffened and Eight Bolt Stiffened connections. In the stiffened connections, triangular stiffeners are required

between the extended endplate and the beam flanges. Each connection type is associated with different beams sizes and design limitations. The main advantage of the endplate connections is the removal of critical field welding from the erection process. When welding critical components in a shop environment higher quality welds can be achieved as opposed to field conditions (Murray et al 2003). Additionally the shop welding of the complete joint penetrated (CJP) welds can accommodate more aggressive erection methods (Murray et al 2003).

Extensive experimental and analytical work on full-scale extended endplate connections was performed during the past three decades. Previous research work and experimental tests were developed to provide guidelines and recommendations for the design of extended endplate connections. Studies on the behavior of extended endplate connections for improving the ductility and strength of the connection were conducted by Krishnamurthy (1979), Tarpy and Cardinal (1981), Murray (1988), Sumner et al. (2002) and Kiamanesh et al. (2012).

Previous studies considered that the endplate thickness is a major parameter that affects the stiffness of the connection and its global response (Kukreti et al. (1987)). Also, continuity plates are often used in extended endplate/column systems to stiffen the column flange and web, in order to resist large forces transmitted by the beam flange. On the other hand, detailing columns without continuity plates reduces the cost and effort needed for fabrication. The deformation contributing from the column flange which causes an additional bolt force in the absence of continuity plates was not explicitly addressed in the design of extended endplate connection. Also, previous work was limited to extended endplate connections having rectangular bolts configuration. Until recently, studies performed by Kiamanesh et al. (2012) and Schweizer (2013)

showed that positioning the bolts in a circular pattern around the flange alters the distribution of the tensile force, and therefore increases the overall capacity and ductility of the connection. Note that no design guidelines and recommendations were proposed for extended endplate having circular bolt configuration.

One of the main behavioral characteristics of extended endplate connections in predicting the ultimate strength and response is the prying phenomenon. Total prying is defined as the amount of tensile force that is added to the bolts due to a significant deformation of extended endplate/column flange system. In particular, secondary prying is defined as the additional force induced in the tension bolts due to excessive column flange deformation (Hantouche et al. (2011)). Several models for predicting the ultimate strength and response are reported in the literature and the important ones include those suggested by Douty and McGuire (1965), Fisher and Struik (1974), Kulak et al. (1987), Jaspart (1991), Bursi and Jaspart (1997), Faella et al. (1997), Swanson (2002), Piluso et al. (2001), Coelho et al. (2004), Eurocode 3(2005), and recently Hantouche et al. (2014). Therefore, it is necessary to develop strength and stiffness models for eight bolted unstiffened extended endplate connections with circular and rectangular bolt patterns.

Strength and stiffness models based on multi-linear spring and beam modeling are developed to predict strength and deformation of isolated components with circular and rectangular bolt configurations. The proposed models are validated against experimental results available in the literature. With its simplicity in application when compared to other numerical methods (i.e. FE analysis), the proposed models are used to design extended endplate connections with circular and rectangular bolt configurations. Based on FE results, the prying phenomenon and bolts response in

extended endplate connections with circular and rectangular bolt patterns are examined. The behavioral characteristics of a typical extended endplate/column system with circular bolts configuration for use in seismic design are investigated.

## CHAPTER II

### PRELIMINARY DESIGN OF EXTENDED ENDPLATE CONNECTION WITH RECTANGULAR AND CIRCULAR BOLT CONFIGURATIONS

#### A. Connection Design

Eight bolted extended endplate connections with circular and rectangular bolt configurations are designed and detailed using guidelines available in the AISC 358-10 (AISC 2010). The extended endplate is welded to the beam and the beam/endplate system is field bolted to the column flange (Figure 1(a)). A rectangular matrix of 8 bolts (2 columns and 4 rows) is provided at the level of each beam flange as shown in Figure 1(b). The connection is designed such that the plastic hinge occurs in the beam at a distance,  $d$ , from the face of the column. Note that the beam and column are made of A992 steel, the plate material is made of A572 with A490 bolts. The beam is designed as a seismically compact element.

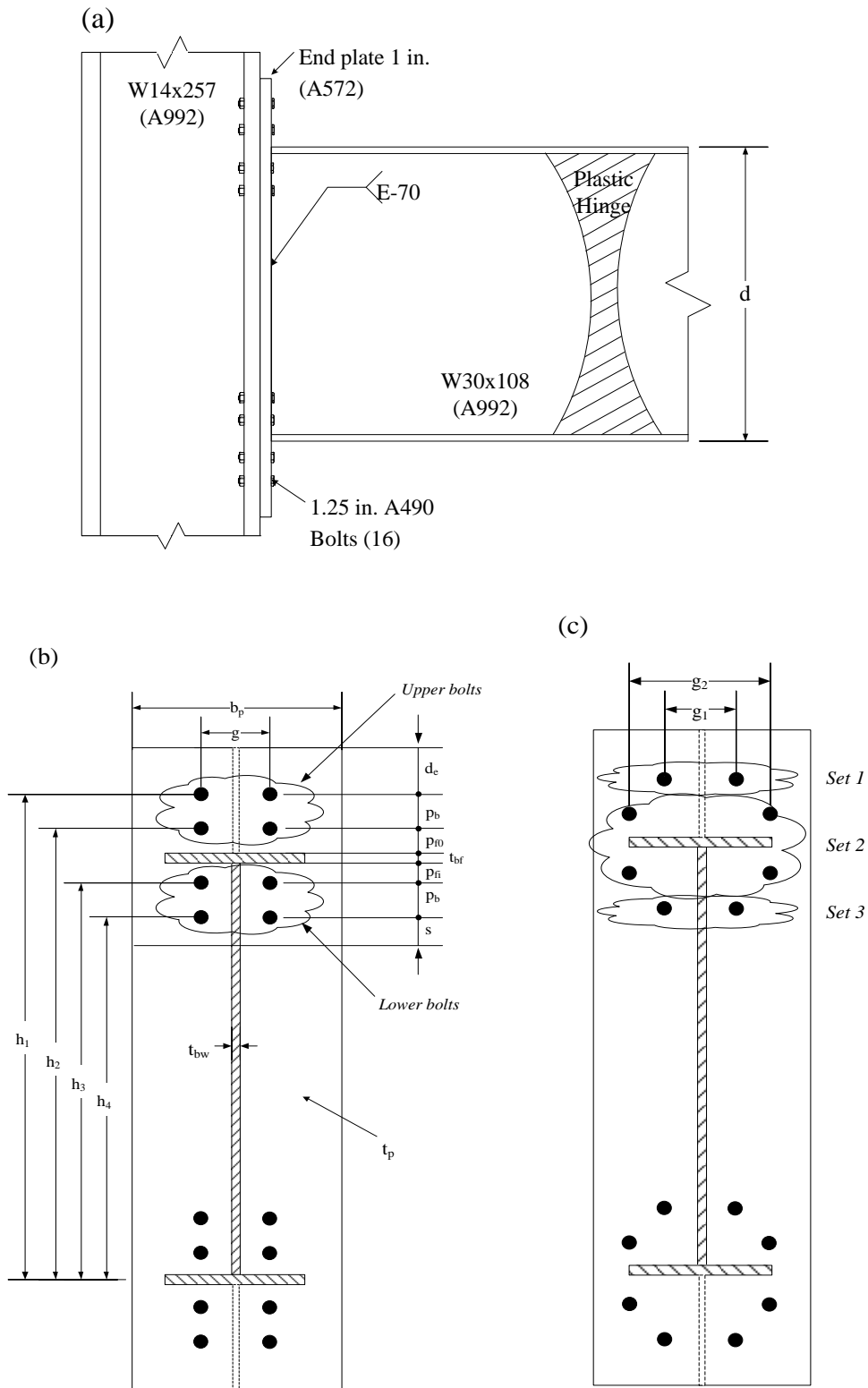


**Figure 1.** (a) Extended endplate Connection (b) Extended endplate with rectangular bolt configuration, (c) Extended endplate with circular bolt configuration

The connections considered in the design consist of W24x76 and W30x108 beams connected to columns with the flange thicknesses,  $t_{cf}$ , varying from 1.9 cm (0.75 in.) to 4.8 cm (1.89 in.). The preliminary connection configuration is based on the following steps:

1. First identify the independent geometric parameters of the extended endplate. Select values for the gauge distances ( $g, p_{fi}, p_{fo}, p_b, d_e, b_p$ ) shown in Figure 1(b) within the range of acceptable values given in table 6.1 of the AISC 358-10 (AISC 2010). After the geometric parameters are defined,  $h_i$  (mm) can be calculated (Figure 1(b)).

2. Assume there is no prying. Determine the minimum bolt diameter  $d_b$  (cm), with capacity to resist the applied moment at the face of the support  $M_f$ .

3. Select the extended endplate thickness,  $t_p$  (mm), based on endplate yielding mechanism. Select the minimum required thickness to the nearest 0.3 cm (1/8 in.).

4. The endplate should not extend from the top of the beam flange by more than 12.7 cm (5 in.), avoiding any local buckling behavior at both edges of the plate.

For the circular bolt configuration, the designer would start with a preliminary rectangular bolt design, and then proceed in accordance to the proposed assumptions and modifications:

1. It is assumed to have equal gage distance ( $p_{fo} = p_{fi}$ ) for the bolts to get a perfectly symmetrical circular configuration.

2. The bolt gage distances shown in Figure 1(c) are calculated as

$g_1 = (b_p - 2e)/2$  and  $g_2 = b_p - 2e$ , where  $b_p$  (cm) is the plate width and  $e$  (cm) is the minimum edge distance defined in section J of the AISC 360-10 (AISC 2010).

3. The 4 far bolts (*Sets 1 and 3*) are moved vertically, rearranged on the circle centered at the beam flange and passing by the bolts in *Set 2* giving a symmetric circular configuration as shown in Figure 1(c).

4. The minimum bolt spacing requirements are in accordance to section J in the AISC 360-10 (AISC 2010).

## **B. Cases Selected for Analysis**

The independent geometric and force related parameters for extended endplate connections are identified. The endplate thickness  $t_p$ , the column flange thickness  $t_{cf}$ , and the bolts vertical gages  $h_i$  reflected by the bolts arrangement are three geometric parameters that impact the amount of prying and deformation in extended endplate connections. The force-related parameter is the applied tension load  $T$  on the extended endplate resulting from the moment applied at the beam tip. The minimum required thickness of the extended endplate,  $t_p$ , was calculated based on the applied moment encountered in the beam. Furthermore, two types of columns were investigated, ranging from rigid columns (column flange is thicker than the endplate), to flexible columns (column flange thinner than the endplate). The study covers columns with flange thicknesses,  $t_{cf}$ , ranging from 1.9 cm (0.75 in.) to 4.7 cm (1.89 in.). Every case is associated with an extended endplate having circular and rectangular bolt patterns to study the effect of bolt distribution on the response. Note that, the endplate thickness,  $t_p$ , is a dependent parameter, incorporated in the design according to the existing design restrictions defined in the AISC 358-10 (AISC 2010).

Therefore, in order to study the amount of total prying in endplate/column systems for a given load  $T$ , a total of twenty eight extended endplates (14 with



rectangular bolts pattern and 14 with circular bolts pattern) are studied and listed in Table 1.

**Table 1.** Test matrix

Column flange thickness, ( $t_{cf}$ )	Endplate thickness ( $t_p$ )	Tension bolt diameter ( $d_b$ )
Design details for W24x76 beam		
1.90 cm ( $\frac{3}{4}$ in.)	2.54 cm (1.00 in.)	2.85 cm ( $1\frac{1}{8}$ in.)
2.15 cm (0.85 in.)	2.54 cm (1.00 in.)	2.85 cm ( $1\frac{1}{8}$ in.)
2.54 cm (1.00 in.)	2.54 cm (1.00 in.)	2.85 cm ( $1\frac{1}{8}$ in.)
3.17 cm ( $1\frac{1}{4}$ in.)	2.54 cm (1.00 in.)	2.85 cm ( $1\frac{1}{8}$ in.)
3.80 cm ( $1\frac{1}{2}$ in.)	2.54 cm (1.00 in.)	2.85 cm ( $1\frac{1}{8}$ in.)
4.44 cm ( $1\frac{3}{4}$ in.)	2.54 cm (1.00 in.)	2.85 cm ( $1\frac{1}{8}$ in.)
4.80 cm (1.89 in.)	2.54 cm (1.00 in.)	2.85 cm ( $1\frac{1}{8}$ in.)
Design details for W30x108 beam		
1.90 cm ( $\frac{3}{4}$ in.)	2.54 cm (1.00 in.)	3.17 cm ( $1\frac{1}{4}$ in.)
2.15 cm (0.85 in.)	2.54 cm (1.00 in.)	3.17 cm ( $1\frac{1}{4}$ in.)
2.54 cm (1.00 in.)	2.54 cm (1.00 in.)	3.17 cm ( $1\frac{1}{4}$ in.)
3.17 cm ( $1\frac{1}{4}$ in.)	2.54 cm (1.00 in.)	3.17 cm ( $1\frac{1}{4}$ in.)
3.80 cm ( $1\frac{1}{2}$ in.)	2.54 cm (1.00 in.)	3.17 cm ( $1\frac{1}{4}$ in.)
4.44 cm ( $1\frac{3}{4}$ in.)	2.54 cm (1.00 in.)	3.17 cm ( $1\frac{1}{4}$ in.)
4.80 cm (1.89 in.)	2.54 cm (1.00 in.)	3.17 cm ( $1\frac{1}{4}$ in.)

## CHAPTER III

### THREE DIMENSIONAL SOLID EXTENDED ENDPLATE MODEL

Using ABAQUS, three-dimensional (3-D) FE models were developed for typical extended endplate connection test specimen which incorporate the following characteristics: (1) nonlinear material behavior for base and bolt material; (2) full pretensioning of fasteners; and (3) contact interaction between the extended endplate and column flange, bolt head and column flange, and bolt nut and endplate.

The FE modeling technique described in this section is to be used (1) for validation against experimental results available in Sumner and Murray (2002) and Schweizer (2013), and (2) for running FE simulations to develop strength and stiffness models that predict the response and strength of extended endplate connection having rectangular and circular bolts arrangement.

#### **A. Mesh Design**

Eight-node linear brick elements with reduced integration (C3D8R) were used to mesh the endplate/column system. Figure 2 shows a full 3-D model representing the extended endplate/column system with rectangular bolts configuration. The length of the column was equal to 305 cm (120 in.).

The model consists of a column, a beam, an endplate and 16 tension bolts. The beam is attached to the endplate using tie constraint representing the CJP welds in order to allow full load transfer between the elements. The tie constraint fuses together two elements having different mesh constitution. The interaction between the plate, bolt

head, bolt shank and column flange are modeled as surface to surface contact with finite sliding and a coefficient of friction equal to 0.2.

## **B. Material Properties**

The von Mises yield criterion is used in the analysis. The bolts were modeled on ABAQUS using their gross area, rather than their effective area. A490 bolts are modeled with a yield stress of 811 MPa (117.5 kips) and an ultimate stress of 872 MPa (126.5 kips). The yield strain, was 0.00405 and the ultimate plastic strain, was 0.03084. The yield and ultimate stress used for the base material are 385 MPa (55 ksi) and 500 MPa (71.5 ksi), respectively. The yield strain used for the base material is 0.00189, and its plastic strain is 0.09827. For all the steel members of the connection, Young's modulus was assumed as  $E=203,000$  MPa (29000 ksi), and Poisson's ratio as  $\nu = 0.30$ . In conclusion, a bilinear model with isotropic hardening for both base and bolt material was used in the analysis.

## **C. Boundary Conditions and Loading**

The analysis was divided into two steps: (1) pretension step, where the 16 bolts are pretensioned to the minimum required force defined in the AISC 360-10 (AISC 2010), and (2) loading step, where the monotonic load is applied at the beam tip. In the pretension and loading steps, the degrees of freedom of the column edge are constrained against any translation and rotation. The lateral sides of the beam flange are assumed to be fixed against translation along the x-direction. The outer and inner faces of the beam flange are fixed against translation in the y-direction to avoid any bending action on the connection (Figure 2). To compute the net primary prying force,  $Q_p$ , the column flange

is assumed to be fully rigid and is fully constrained against any translation and rotation. However the column flange is free to deform when computing the total prying force,  $Q_T$ . During the first step, the pretensioning force is generated by applying a bolt force on the shank equal to the minimum pretension force. Throughout the loading step, surface pressure is applied on the flange section at the beam tip.

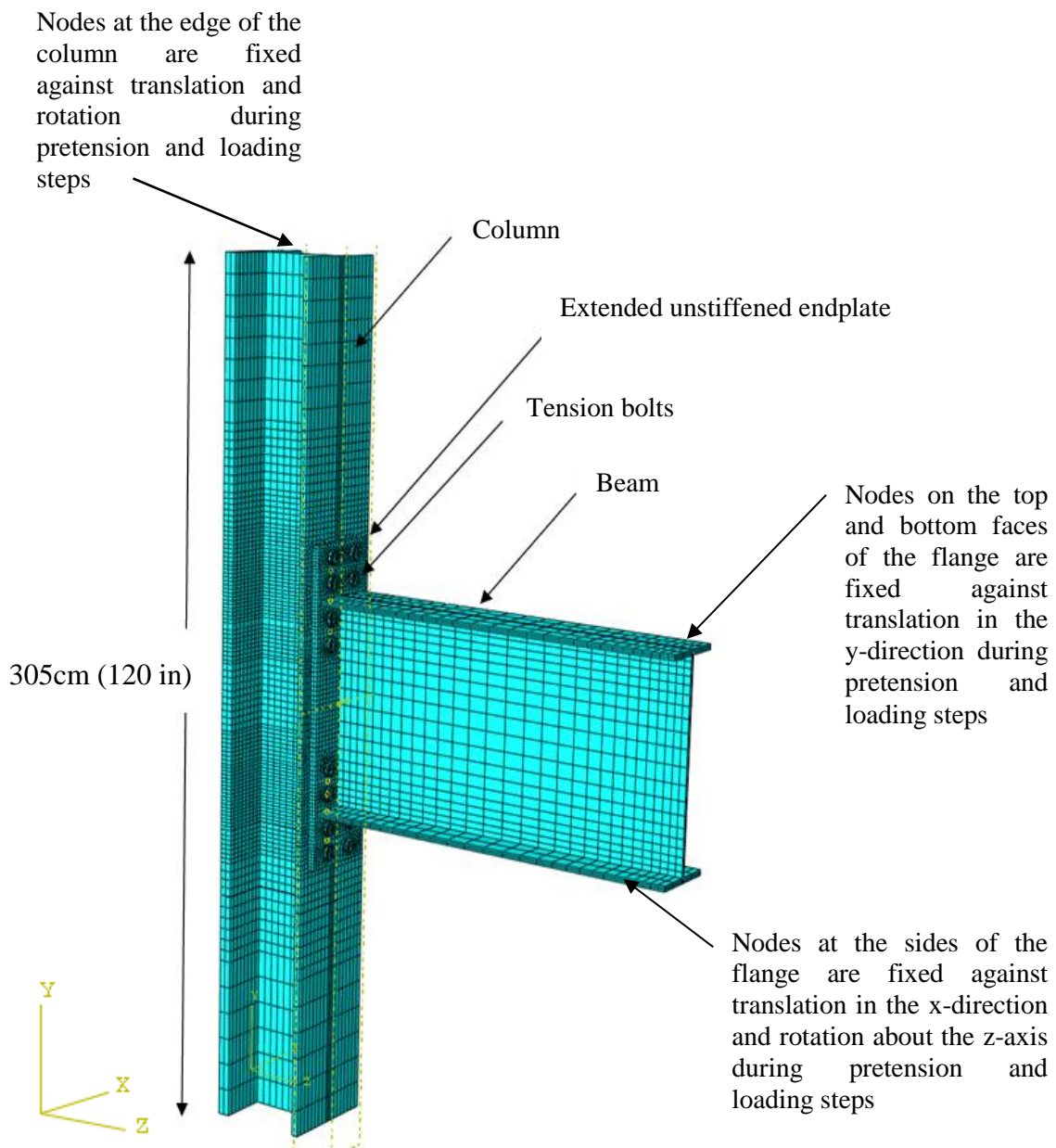


**Figure. 2.** Three-dimensional model of endplate connection with rectangular bolt configuration

#### **D. Validation with Experimental Results**

Two FE models of extended endplate connections with rectangular and circular bolt configurations were developed to reproduce experimental results available in the literature. Figures 3(a) and 3(b) show a comparison of the FE moment-rotation curve with experimental results of Sumner et al. (2002) and Schweizer (2013), respectively. The FE model predicts with excellent agreement the experimental moment-rotation envelope curve as far as stiffness, strength and ductility. Hence, FE models can be used to develop extended endplate models with rectangular and circular bolt configurations for the parametric study.

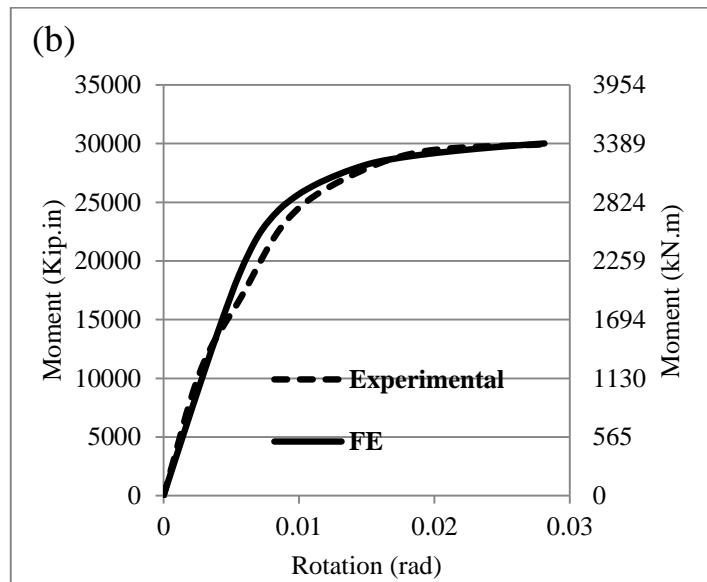
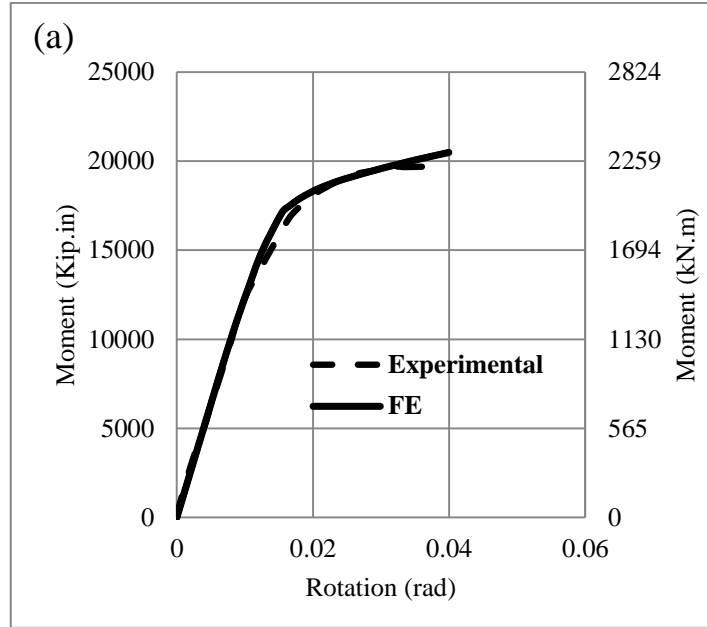


**Figure 3.** (a) Extended endplate with rectangular bolt configuration moment-rotation curves (Sumner et al. (2013)) and (b) extended endplate with circular bolt configuration moment-rotation curves (Schweizer (2013)).

## CHAPTER IV

### INVESTIGATION OF PRIMARY AND SECONDARY PRYING

This study investigates the prying phenomenon in extended endplate/column systems with circular and rectangular bolt configurations that should be addressed in designing full-strength connections. More importantly, this study highlights the effect of the circular bolt arrangement on prying forces in extended endplate connections.

#### A. Data Analysis

The prying force is calculated at the step where the first bolt row fails causing the failure of the connection. The bolt force exhibited in every bolt  $B$  is calculated by multiplying the von Mises stresses by the gross section area of the bolt shank. The prying force,  $Q$ , is calculated by subtracting the total bolt force  $B$  from the total applied force,  $T$ , at failure:  $Q = B - T$ . Two models were generated on ABAQUS to calculate the secondary prying,  $Q_s$ . In the first model, the column flange is free to deform used to calculate the total prying,  $Q_T$ . The second model was developed to calculate the primary prying  $Q_P$  with rigid column flange. The percentage secondary prying ( $Q_s / T$ ) is obtained by subtracting the primary prying ( $Q_p / T$ ) from the total prying ( $Q_T / T$ ) at the same load step  $T$  where failure occurs, as shown in Eqn 1.

$$\left(\frac{Q_s}{T}\right) = \left(\frac{Q_T}{T}\right) - \left(\frac{Q_p}{T}\right) \quad (1)$$

## B. Prying Phenomenon

FE models of extended endplate connection with various column flange thicknesses having circular and rectangular bolt configurations were analyzed under monotonic loading. The primary and secondary prying percentages were calculated for each column flange thickness associated with W24x76 and 30x108 beams as shown in Table 2.

**Table 2.** Percentage of primary and secondary prying W24x76 and W30x108 beams

		<b>W24x76</b>		<b>W30x108</b>	
$t_{cf}$ (cm)	Percent prying (%)	Circular	Rectangular	Circular	Rectangular
1.9	Primary	85	60	100	66
	Secondary	34	39	43	54
2.1	Primary	72	50	90	66
	Secondary	28	30	36	47
2.5	Primary	60	43	69	55
	Secondary	25	26	32	39
3.2	Primary	58	48	71	56
	Secondary	7	9	13	18
3.8	Primary	59	57	65	53
	Secondary	0	0	10	14
4.4	Primary	58	57	65	52
	Secondary	0	0	7	11
4.8	Primary	57	57	66	57
	Secondary	0	0	0	0

The extended endplate/column system with circular bolt configuration exhibited higher total prying forces for all the studied cases. The total prying exhibited from the system is the added contribution of primary prying (generated from the plate



deformation) and secondary prying forces (induced by the excessive column flange deformation). Endplate connections with circular bolt pattern associated with W24x76 and W30x108 beams exhibited lower secondary prying forces (Table 2). On the other hand, endplate with rectangular bolt configuration exhibited lower primary prying forces when compared to its circular counterpart. More generally, as the column flange thickness increases, the secondary prying force decreases in both endplates with circular and rectangular bolt configurations.

### C. Bolt Force Variation

To further investigate the effectiveness of the circular bolt pattern, the bolt force history was investigated for extended endplate connections having circular and rectangular bolt configurations with  $t_{cf}$  equal to 2.1, 2.5, 3.8 and 4.8 cm as shown in Figure 4. It can be seen that for all column/endplate system with circular bolt configurations, the far bolts (*Bolts 4*) are involved in carrying the load earlier and more effectively than *Bolts 4* in rectangular bolt configurations. In connections with circular bolt pattern, the far bolts (*Bolt 4*) carry more load than the near bolts (*Bolts 2 and 3*), which are subject to higher bending moments in rectangular bolt configuration and carry more load than the other bolts (*Bolt 1, 4*). In rectangular bolt configuration, *Bolts 3* and *4* follow the same loading history, since their curves overlap. The two bolts are stiffened by the beam web; they are subject to equal deformations and stress distribution. In contrast, in connections with circular bolt configuration the force is equally spread across the bolts.

Furthermore, in connections with rectangular bolt configurations where  $t_{cf} = 4.8$  cm, the unstiffened far bolt (*Bolt 1*) carries no force when the beam is loaded, while

in its counterpart connection with circular bolt configuration, all bolts are engaged. Hence in circular connection, the load is efficiently spread across the bolts, developing a more ductile behavior. Based on FE results, the near bolts, *Set 2* (Figure 1(c)) are fully effective in connections with rectangular bolt configuration, while the four far bolts, *Sets 1 and 3*, achieve up to 80% of their tensile strength. The bolt force of the sixteen tension bolts was calculated as a percentage of their ultimate tensile strength. In the circular bolt pattern, the bolts are more effective and reach higher capacity than the bolts in the connection with rectangular bolt configurations.

Finally, in connections with rectangular and circular patterns *Bolt 1* exhibited similar bolt force history in thin columns. However, the near bolts (*Bolts 2 and 3*) become more effective and reach their ultimate capacity with thicker columns ( $t_{cf} = 4.8$  cm).

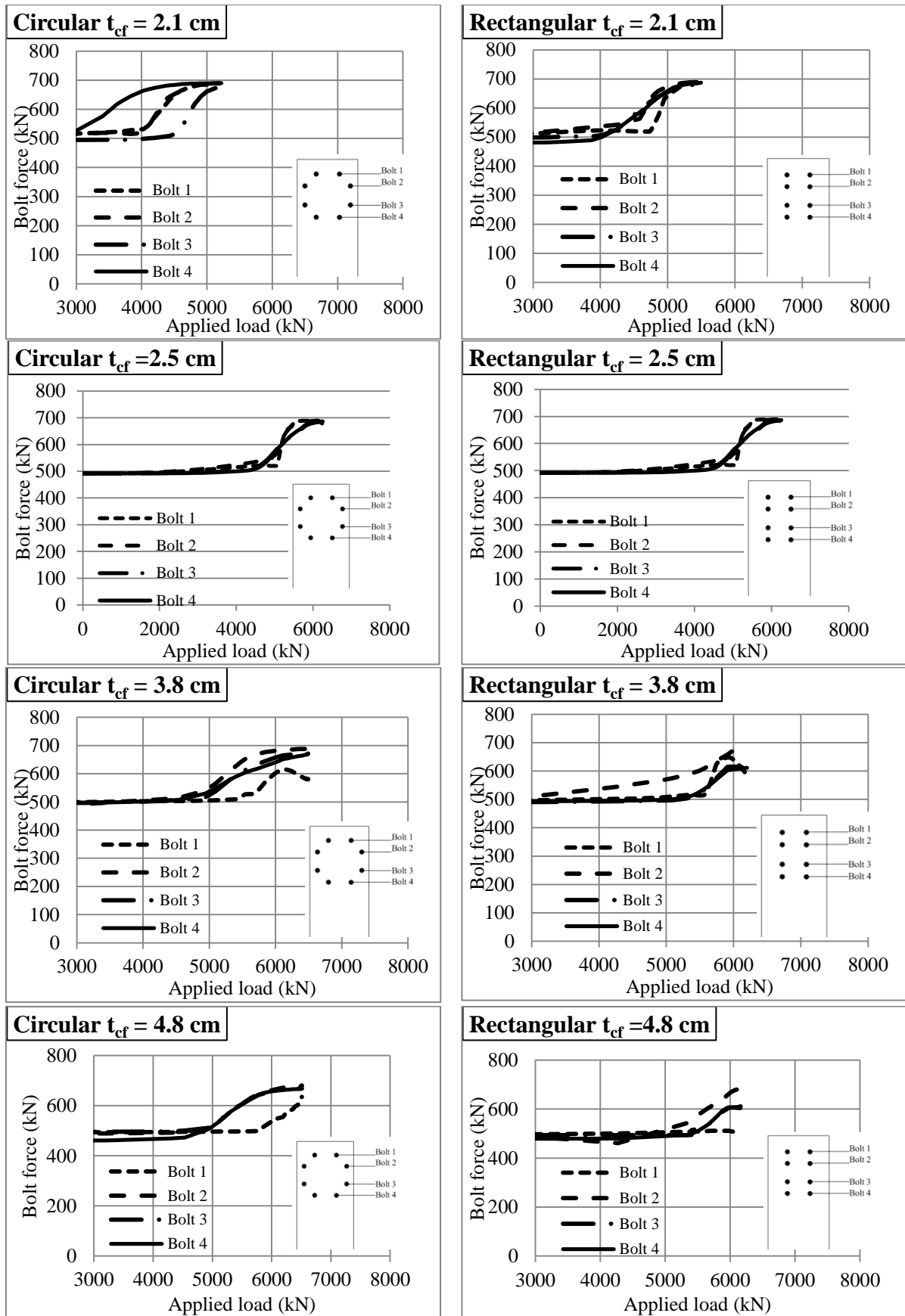


**Figure. 4.** Bolt force history for extended endplate with rectangular and circular bolt configurations

## CHAPTER V

### STRENGTH MODELS

The FE and experimental results are used to develop strength models to predict the capacity of extended endplate and column flange with circular and rectangular bolt configurations. Four possible failure modes are addressed: (1) formation of a plastic hinge at the K-zone followed by fracture of the interior tension bolts, (2) formation of a plastic hinge at the first bolt line followed by fracture of the interior tension bolt, (3) full plastification, and (4) pure tension bolt fracture.

#### **A. Strength Models for Circular Bolts Configuration**

##### ***1. Extended Endplate with Circular Bolt Configuration***

Strength models for extended endplate connections with circular bolt configuration were not addressed in previous studies. The FE results show that extended endplate connection with circular bolt configuration exhibit high primary prying force, hence it is deemed necessary to quantify the endplate's capacity. The endplate was modeled as strip beam element for the plate, and springs to model the bolts. The von Mises stress contours obtained from the FE analysis of the selected cases show that no full plastification of the extended endplate at the K-zone is developed. Thus, the problem is considered statically indeterminate and an additional relationship that relates the prying force to the applied load is needed to solve the problem. A partial yielding model for extended endplate connections with circular bolt configuration is needed to predict the endplate capacity.

A detailed parametric study was performed to limit the range of endplate partial yielding. Geometric parameters that impact the plate yielding are found to be the radius of the concentric bolt pattern,  $r$ , and the thickness of the plate,  $t_p$ . From the FE results, partial yielding developed in extended endplate with  $t_p$ , ranging from 3 cm (1.2 in.) to 4.3 cm (1.7 in.). A dimensionless ratio which involves the radius of the concentric bolts to the plate thickness  $r/t_p$  has a major impact on the amount of yielding encountered in the plate. Five endplate FE models were analyzed and a linear relationship can be fitted to the FE results to obtain an analytical model for prediction of the primary prying force when partial yielding occurs followed by bolt fracture. The best fit linear equation obtained for  $2.80 \leq r/t_p \leq 5.00$  is:

$$\frac{Q_p}{T} = 24 \left( \frac{r}{t_p} \right) - 54 \quad (2)$$

Considering the bolt force equal to  $\gamma B_n$ , and by substituting  $B=Q+T$  in Eqn 2 the capacity per bolt can be written as follows:

$$T = \frac{\gamma B_n}{0.24 \left( \frac{r}{t_p} \right) + 0.46} \quad (3)$$

where  $\gamma$  is assumed to be equal to 0.8 to account for bending of the tension bolts and  $B_n$  (kN) is the nominal bolt tensile strength. Note that the bolts are not only subject to tension forces but are also subject to bending. The proposed strength model is validated against previous work performed by Kiamanesh et al. (2013) and predicts a capacity of 3,552 kN (800 kips) for W30x99 beam with  $r/t_p = 4.87$ . This is around 4.7% difference when comparing with the FE results. Hence the proposed model

predicts with excellent agreement the capacity of the extended endplate with circular bolt configuration.

## 2. Column Flange with Circular Bolt Configuration

The 8 tension bolts were divided into three *Sets* according to their behavior as shown in Figure 1(c). The proposed strength model consists of a spring representing the bolts and a beam element for the column flange as shown in Figure 5(a).

The FE models cover the range of column flange thicknesses varying from 1.9 cm (0.75 in.) to 4.8 cm (1.89 in.). For thin column flanges where  $t_{cf}$  is less than 2.54 cm (1 in.), flange mechanism occurs in *Sets 1* and *3*, and mixed mode failure occurs in *Set 2*. However for thick column flanges, where  $t_{cf}$  is greater than 2.54 cm (1 in.), mixed mode failure occurs in *Sets 1, 2* and *3*. Mixed mode failure develops in stiffer columns and the capacity is calculated as follows:

$$T = T' = \frac{\gamma B_n n}{m + n} + \frac{M_p}{m + n} \quad (4)$$

and for flange mechanism:

$$T = T' = \frac{(1 + \delta) M_p}{m} \quad (5)$$

where:

$$\delta = 1 - \frac{d_h}{p} \quad (6)$$

$$M_p = \frac{p t_{cf}^2}{4} F_y \quad (7)$$

where,  $T$  (kN) is the applied force,  $M_p$  (kN.m) is the plastic moment,  $d_h$  (cm) is the bolt hole diameter,  $p$  (cm) is the tributary width of a pair of tension bolts,  $F_y$  (MPa)

is the yield stress,  $m$  (cm) is the length of the column flange measured from the inside edge of the bolt to the location of occurrence of the plastic hinge at the K-zone,  $n$  (cm) is the length measured from the inside edge of the bolt line to the outside edge of the column flange, where contact with the endplate occurs as shown in Figure 5(a), and  $\delta$  is the ratio of the net area at the center of the bolt line to the area of the beam flange. The bolt force is assumed to be applied at a distance  $d_b / 2$  from the bolt hole centerline (Kulak et al. (1987)). The tributary width per bolt,  $p$ , used in computing the plastic moment,  $M_p$ , is reflected by the vertical length of the column,  $W_c$ , that deflects when the load is applied. The deformed length varies with the column flange thickness; the thicker the column flange the smaller the deformation. Therefore, there is no average length that can be considered to compute  $W_c$ , thus a linear relationship between  $W_c$  and  $t_{cf}$  is derived as:

$$W_c = -40t_{cf} + 195 \geq 142 \text{ cm} \quad (8)$$

A linear relationship is obtained from the best fit of the FE results for the studied cases. The tributary width,  $p$ , can be calculated as follows:

$$p = \frac{17W_c - 835}{n_b} \text{ (cm / bolt)} \quad (9)$$

The proposed strength model predicts a capacity of 5,843 kN for W30x99 beam associated with W14x194 thick column having a  $t_{cf}$  equal to 3.65 cm (1.43 in.) studied in Kiamanesh et.al (2013). This is around 1% less than the reported results. The proposed strength model predicts with excellent agreement the capacity of the column flange with circular bolt configuration.

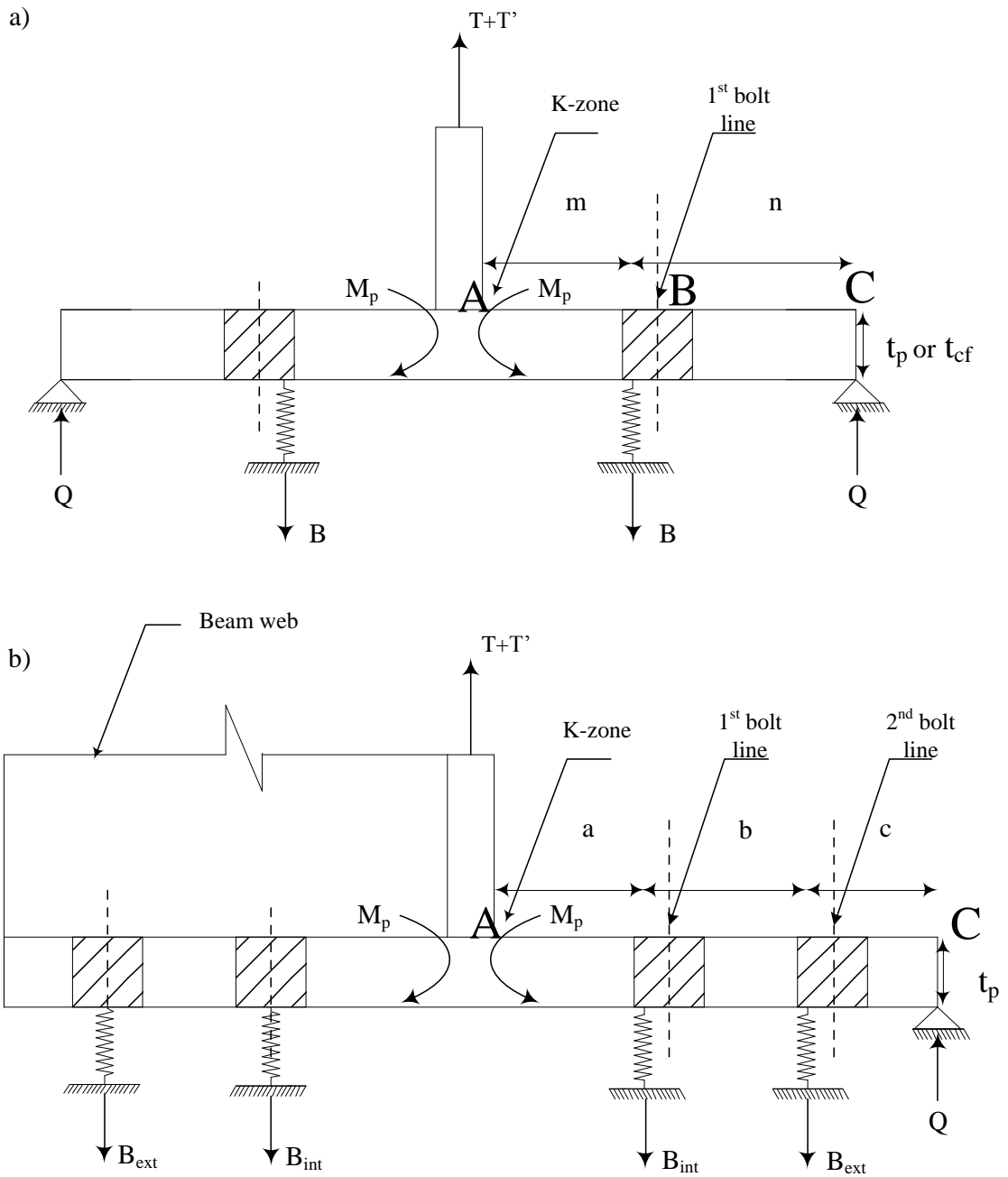


**Figure. 5.** (a) End plate with circular bolt or column flange with circular and rectangular bolt configurations geometry, (b) endplate with rectangular bolt configuration geometry



## B. Strength Models for Rectangular Bolt Configuration

### 1. Extended Endplate with Rectangular Bolt Configuration

A strength model is developed to predict the primary prying capacity exhibited in the extended endplate with rectangular bolt configuration. Two vertical strips were modeled at the level of each flange as shown in Figure 5(b), accounting for the beam web stiffening effect. At failure of the connection, mixed mode occurs at the *upper bolts* lines (Figure 1(b)). However, at the *lower bolts* level, (Figure 1(b)), the beam web acts as a stiffener, hence the bending of the plate is negligible, and the plate separates completely from the column flange as shown in Figure 6. Therefore, the force developed at the *lower bolts*,  $T'$ , is equal to:

$$T' = \gamma_b \xi B_n / 8 \quad (10)$$

where the reduction factor ( $\xi = 0.75$ ) is used to account for the beam web stiffening effect and  $n_b$  is the number of the tension bolts. The strength associated with the *upper bolts* is derived from previous models available in the literature. For mixed mode failure at the *upper bolts* level (plastic hinge develops at the K-zone followed by interior bolt fracture):

$$T = \frac{\gamma B_n c}{a + b + c} + \frac{\gamma B_n (b + c)}{a + b + c} + \frac{M_p}{a + b + c} \quad (11)$$

$$M_p = \frac{pt_p^2}{4} F_y \quad (12)$$

$$p = \frac{8b_p}{n_b} \quad (13)$$

where,  $T$  (kN) is the applied forces,  $a$  (cm) is the length of the plate measured from the inside edge of the interior bolt to the location of occurrence of the plastic hinge at the K-zone,  $b$  (cm) is the gage distance between the tension bolts, and  $c$  (cm) is the

length measured from the inside edge of the exterior bolt line to the outside edge of the endplate as shown in Figure 5(b). The proposed strength model results, revealed a capacity of 5,931 kN and 5,514 kN for extended endplate with rectangular bolt configuration associated with W30x108 and W24x76 beams, respectively. This is around 1% and 8% more than the strength predicted by the FE results. For validation purposes, the proposed model is validated against FE simulations reported in Kiamanesh et al. (2013). The proposed model predicts a capacity of 3,383 kN. The percentage difference is around 3.5% when compared with results available in Kiamanesh et al. (2013), for the extended endplate ( $t_p = 2.54$  cm) associated with W30x99 beam.

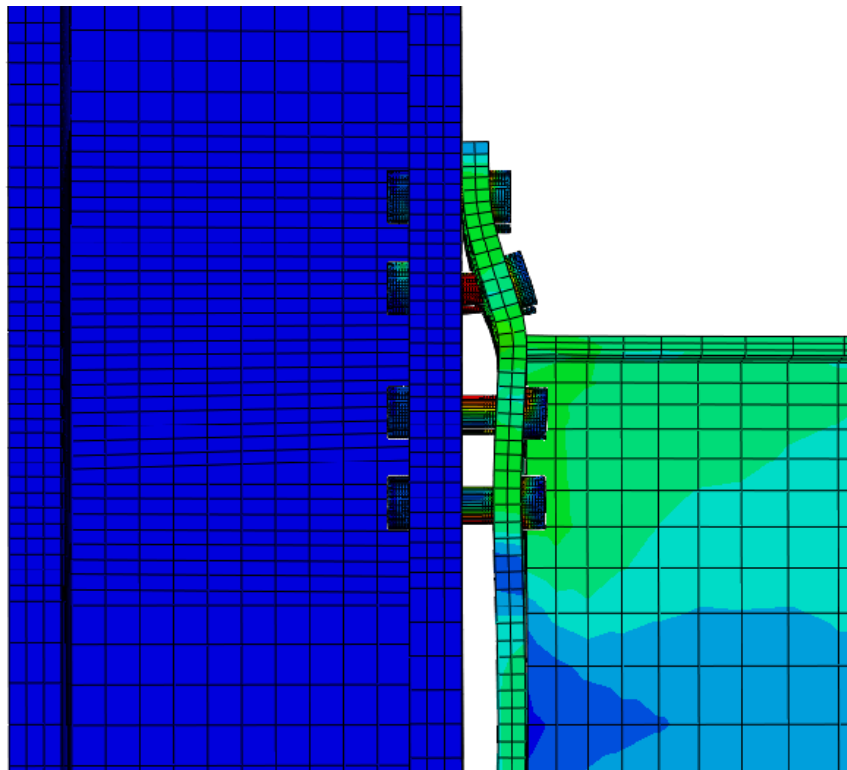


**Figure. 6.** Deformation of the extended endplate with rectangular bolt configuration

## 2. Column Flange with Rectangular Bolt Configuration

The column flange is subdivided into 4 horizontal strips consisting of 2 bolts each as modeled in Figure 5(a). From the FE results, the governing failure modes are: (1) full plastification of the flange followed by bolt fracture, and (2) tension bolt fracture. Full flange plastification occurs when  $t_{cf}$  varies between 1.9 cm (0.75 in.) to 3.2 cm (1.25 in.) and tension bolt fracture occurs when  $t_{cf}$  varies between 3.2 cm (1.25 in.) to 4.8 cm (1.89 in.), where complete plate separation occurs. The capacity for tension bolts fracture, when full separation occurs, can be calculated as  $T = T' = \gamma \xi B_n$ , and when full plastification occurs (plastic hinge develops at the K-zone followed by plastification of interior and exterior bolt lines):

$$T = T' = \frac{(1 + \delta)M_p}{m} \quad (14)$$

where  $p$  is calculated as per Eqn 9,  $m$  (cm) is the length of the column flange measured from the inside of the bolt to the location of the plastic hinge at the K-zone as shown in Figure 5(a).

The proposed strength model predicts a capacity of 5,260 kN for a W30x108 beam connected to a W14x194 column which is 7% more when comparing with the FE results. In addition the model predicts a capacity of 5,336 kN (1,202 kips) for a W14x257 column connected to a W24x76 beam, which is 4 % more when comparing with the FE results. Hence, the proposed strength model predicts with reasonable agreement the capacity of the column flange associated with deep beams when compared with the FE results.

## CHAPTER VI

### COLUMN FLANGE STRENGTH PREDICTION USING YIELD-LINE ANALYSIS

The yield-line theory was first introduced in 1962 and used in reinforced concrete slabs. Later on, the principles behind the theory have been applied in the analysis of steel plate yielding. A yield line is defined as the continuous formation of plastic hinges along a line. The plastic moment,  $M_p$ , at which the plastic hinges form remains relatively constant along the line as the deformations increase, thus forming a visible yield line. Since the plastic deformations at the yield lines are significantly larger than the elastic deformations in the regions between yield lines, it is supposed that these elastic regions behave as rigid plates. In yield line theory, failure occurs when the formation of yield lines in a plate form a collapse mechanism. This formation of yield lines is referred to as a yield line pattern. The yield line pattern divides the total plate into various solid regions.

There are several guidelines that should be followed in order to establish the location of a yield line;

1. Axes of rotation generally lie along stiff lines of support.
2. Yield lines pass through the intersection of the axes of rotation of adjacent plate segments.
3. Along every yield line, the bending moment is assumed to be constant and is taken as the plastic moment of the plate  $m_p$ .
4. Yield lines between adjacent rigid regions pass through the point of intersection of the axis of rotations of the two regions.

In this section, a yield-line analysis is developed to predict the column flange yield strength with circular and rectangular bolt patterns. A governing yield-line mechanism is identified for each bolt configuration. The virtual work method is used to compute the energy dissipation of a given yield-line pattern. The virtual work method is based on the principle of conservation of energy. The external work  $W_e$  done by the applied loads from a unit virtual displacement is set equal to the internal work,  $W_i$ , done to accommodate these displacements as the flange rotates about the yield lines. Each unique yield line pattern will result in a different required plastic capacity for a known applied load. The pattern that requires the largest capacity (flange thickness) is the controlling pattern.

The internal work stored in a particular yield line mechanism is the sum of the internal energy stored in each yield line forming the mechanism. The internal energy stored in any given yield line is obtained by multiplying the normal moment on the yield line with the normal rotation of the yield line.

### A. Circular Bolt Configuration

Based on yield-line theory discussed earlier and FE results, the governing yield-line pattern for column flange having circular bolt configuration is presented in Figure 7 (a). The internal work  $W_i$  can be computed as follows:

$$W_i = 2M_p \left[ 4 \left( \frac{b_{cf}}{2} \times \frac{1}{s} \right) + 4(l + 2p_b) \frac{1}{g_2} + 8(p_b + s) \frac{1}{g_1} \right] \quad (15)$$

Where  $b_{cf}$ ,  $s$ ,  $l$ ,  $p_b$ ,  $g_2$ ,  $g_1$ , are geometric parameters defined in Figure 7 (a). The external work done by the system is equal to  $W_e = F_u \cdot 1$ . where  $F_u$  is equal to the ultimate load at failure. The connection strength based on yielding of the column flange is found

by equating the external energy with the internal energy. The minimum required column flange thickness,  $t_{cf}$  is computed as follows:

$$t_{cf} \geq \sqrt{\frac{F_u}{\left[2\left(\frac{b_{cf}}{2} \times \frac{1}{s}\right) + 2(l + 2p_b)\frac{1}{g_2} + 4(p_b + s)\frac{1}{g_1}\right]F_{yc}}} \quad (16)$$

where  $F_{yc}$  (MPa) is the yield stress of the column. According to Eqn 16, the required minimum column flange thickness for extended endplate associated with W30x108 beam connected to a W14x257 column is computed as  $t_{cf} \geq 3.48$  cm (1.37 in.).

The distance  $s$ , can be calculated by differentiating the internal work with respect to  $s$

and equating to zero:  $s = \frac{1}{2} \sqrt{b_{cf} \times g_1}$

According to the AISC 358-10 (AISC 2010), the required minimum column flange thickness for the same connection is computed as  $t_{cf} \geq 2.90$  cm (1.14 in.).

## B. Rectangular Bolt Configuration

According to the AISC 358-10, the governing yield line pattern which requires the highest yield capacity for the unstiffened column flange having a rectangular bolt holes pattern is shown in Figure 7 (b).

According to the principle of conservation of energy, the connection strength based on yielding of the column flange is found by equating the external energy with the internal energy ( $W_i = W_e$ ) resulting in the minimum required column flange thickness:

$$t_{cf} \geq \sqrt{\frac{F_u}{\left[\left(b_{cf} \times \frac{1}{s}\right) + 4(c + 2p_b + s)\frac{1}{g}\right]F_{yc}}} \quad (17)$$

where  $F_{yc}$  (MPa) is the yield stress of the column. According to Eqn 17, the required minimum column flange thickness for extended endplate associated with

W30x108 beam connected to a W14x257 column is computed as  $t_{cf} \geq 2.92 \text{ cm (1.14 in.)}$ .

The distance,  $s$ , is found by differentiating the internal work equation  $W_i$  with respect to

$s$  and setting the resulting equation equal to zero, giving:  $s = \frac{1}{2} \sqrt{b_{cf} \times g}$ .

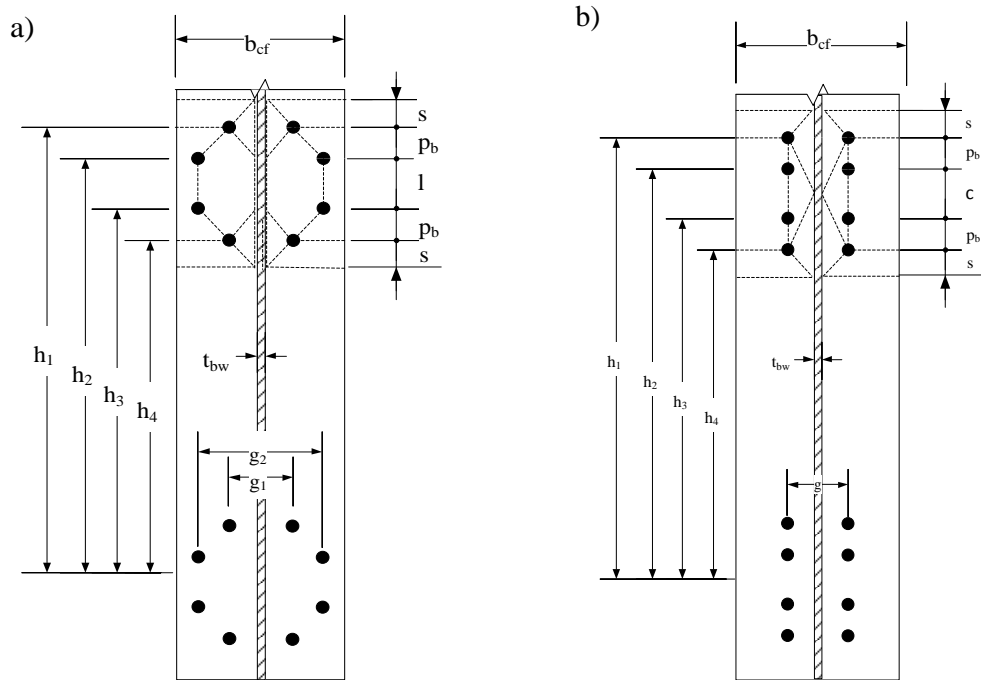


**Figure. 7.** Yield line mechanism for column flange with (a) circular bolt configuration, (b) rectangular bolt configuration

## CHAPTER VII

### STIFFNESS MODELING

The experimental and FE results of extended endplate connections with circular and rectangular bolt configurations are used to develop a stiffness model. The model is based on multi-linear springs which model deformations of key component elements from tension bolt elongation, bending of the plate, column flange deformation including primary and secondary prying forces. Modeling the endplate is complex because all of these mechanisms interact with one another and hence simple strength checks cannot provide the necessary stiffness, ductility information required for seismic design.

#### **A. Bolt Stiffness Model**

The bolt stiffness model proposed by Hantouche et al. (2013) is used to model the tension bolts throughout the loading history of the extended endplate. The bolt stiffness model is composed of four linear segments. The first segment models the bolt in the pretension step, the second segment models the bolt in the elastic range, the third segment models the bolt after first yielding has been reached and the fourth segment models the bolt in the plastic range. The elastic bolt stiffness  $K_b$  (kN/cm) is calculated as follows (Swanson (1999))

$$\frac{1}{K_b} = \frac{fd_b}{A_b E} + \frac{L_s}{A_b E} + \frac{fd_b}{A_{be} E} \quad (18)$$



where,  $f$  is the stiffness correlation factor,  $A_b$  ( $\text{cm}^2$ ) is the nominal area of the bolt shank,  $A_{be}$  ( $\text{cm}^2$ ) is the effective area of the threads and  $L_s$  (cm) is the free shank length of the bolt.

## **B. Extended Endplate/Column System with Circular Bolt Configuration**

### ***1. Extended Endplate with Circular Bolt Configuration***

The proposed stiffness model consists of the extended endplate associated with deep beams having an endplate thickness,  $t_p$ , less than 3.00 cm (1.2 in.). From the FE results, full plastification develops at the *upper bolt* line (Figure 1(b)), followed by endplate separation at the *lower bolts* level at failure of the bolts. A decision tree showing different endplate limit states (*Upper bolts* strip) is shown in Figure 8(a).

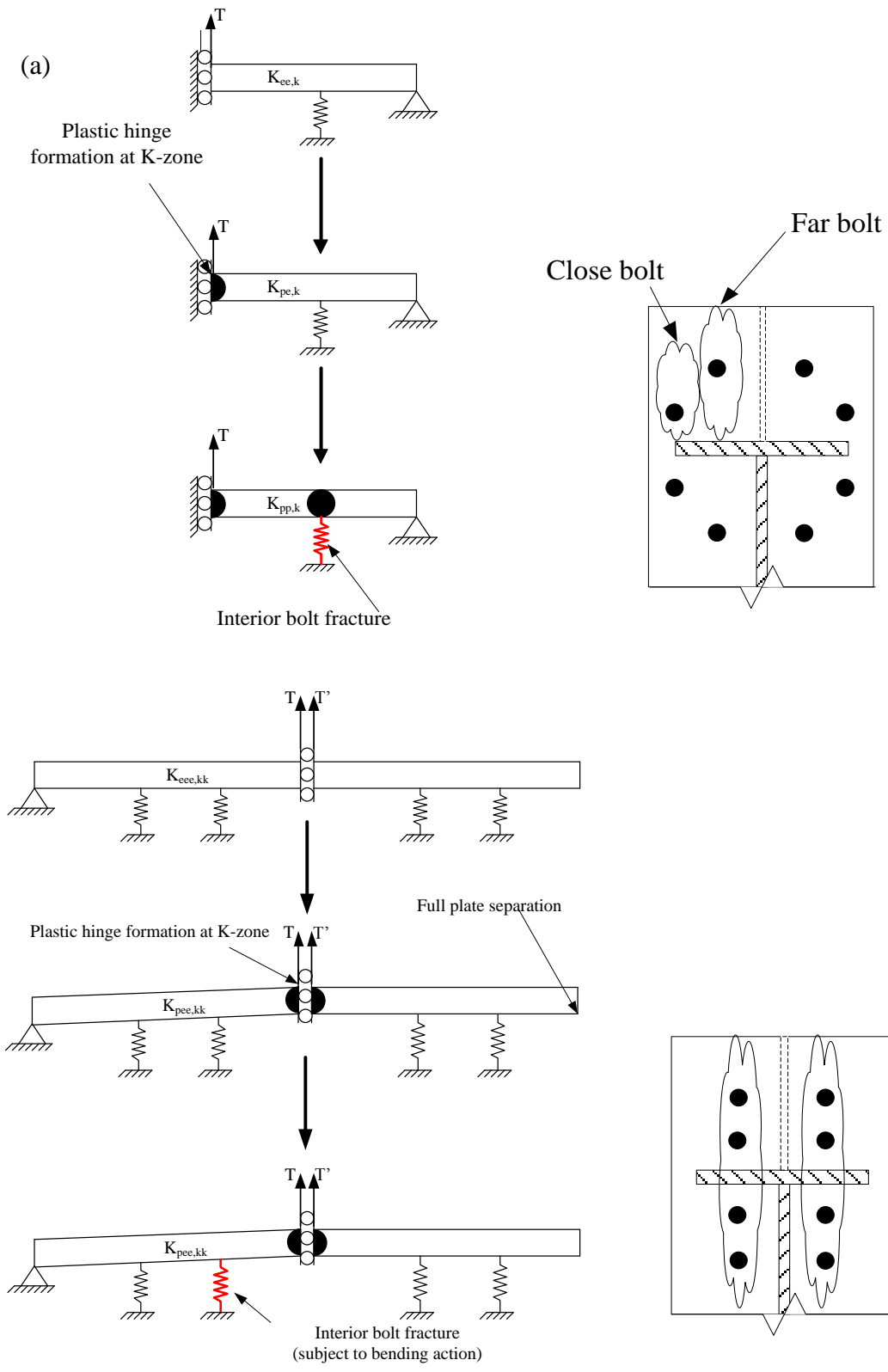


**Figure 8.** (a) Decision tree for extended endplate with circular bolt configuration and (b) Decision tree for extended endplate with rectangular bolt configuration

At the *upper bolts* level shown in Figure 1(b), the stiffness model was developed in accordance to the far bolts geometry (Figure 5(a)). The subscript used in the stiffness coefficients reflects the state of the endplate and *upper bolt*. For instance,  $K_{ee,k}$  is the stiffness of the endplate that is totally elastic, with the bolt in its  $k^{\text{th}}$  state.  $K_{pe,k}$  is the stiffness of the endplate when the plastic hinge has formed at the K-zone and the bolt line is still in its elastic range,  $K_{pp,k}$  is the final stiffness of the endplate when the bolt line and the K-zone are in their plastic state and full plastification occurs in the endplate. The stiffness was derived using direct stiffness method and is presented in the following equations accounting for shear deformation. Strain hardening which occurs after plastic hinge formation was modeled by a rotational spring with constants  $K_{h1}$  and  $K_{h2}$  according to Douty (1964). The hinge depth was set equal to the thickness of the endplate. The mechanistic equations are developed below:

$$K_{ee,k} = \frac{12EI(3EI + K_{b,k}\Omega_3)}{\gamma_{ee,k}} \quad (19)$$

$$Q_{ee,k} = \frac{18EI(K_{b,k}mn^2\beta_b - 2EI)}{\gamma_{ee,k}} \quad (20)$$

$$\gamma_{ee,k} = 12EI\Omega_1 + K_{b,k}\Omega_2 \quad (21)$$

$$K_{pe,k} = \frac{12EI(3EI(K_{b,k}n^2 + K_{h1}) + K_{b,k}K_{h1}\Omega_3)}{\gamma_{pe,k}} \quad (22)$$

$$Q_{pe,k} = \frac{18EI(2EI(K_{b,k}mn - K_{h1}) + K_{b,k}K_{h1}nm^2\beta_b)}{\gamma_{pe,k}} \quad (23)$$

$$\gamma_{pe,k} = 12EI(K_{h1}\Omega_1 + K_{b,k}(m^3n^2\beta_a + m^2n^3\beta_b) + 3EI\Omega_4) + K_{b,k}K_{h1}\Omega_2 \quad (24)$$

$$K_{pp,k} = \frac{K_{h1}K_{h2} + K_{b,k}n^2(K_{h1} + K_{h2})}{\gamma_{pp,k}} \quad (25)$$

$$Q_{pp,k} = \frac{K_{h2}(K_{b,k}mn - K_{h1})}{\gamma_{pp,k}} \quad (26)$$

$$\gamma_{pp,k} = K_{h2}\Omega_4 + K_{h1}n + K_{b,k}m^2n^2 \quad (27)$$

where

$$\Omega_1 = \beta_b(m^3 + 3nm^2 + 3n^2m) + n^3\beta_a \quad (28)$$

$$\Omega_2 = 3n^2m^4\beta_b^2 + 4n^3m^3\beta_a\beta_b \quad (29)$$

$$\Omega_3 = n^3\beta_a + 3n^2m\beta_b \quad (30)$$

$$\Omega_4 = n^2 + 2mn + m^2 \quad (31)$$

$$p = \frac{b_p}{4} \quad (32)$$

$$I = \frac{pt_p^3}{12} \quad (33)$$

$$\beta_a = 1 + \frac{12EI}{Gpt_p n^2} \quad (34)$$

$$\beta_b = 1 + \frac{12EI}{Gpt_p m^2} \quad (35)$$

$$K_{h1} = \frac{EI}{t_p} \quad (36)$$

$$K_{h2} = \left(1 - \frac{d_h}{p}\right) \frac{EI}{t_p} \quad (37)$$

where  $I$  ( $\text{cm}^4$ ) is the moment of inertia,  $G$  ( $\text{kN}/\text{cm}^2$ ) is the shear modulus of elasticity,  $K_{b,k}$  ( $\text{kN}/\text{cm}$ ) is the bolt stiffness at the  $k^{\text{th}}$  step,  $\beta_a$ ,  $\beta_b$ ,  $\Omega_1$ ,  $\Omega_2$ ,  $\Omega_3$  and  $\Omega_4$  are constants used in the calculation of the extended endplate stiffness and  $\gamma_{ee,k}$ ,  $\gamma_{ep,k}$  are constants used in the calculation of  $K_{ee,k}$ ,  $m$  (cm) is the length of the endplate measured from the inside edge of the bolt line to the K-zone and  $n$  (cm) is the length of the

endplate measured from the inside edge of the bolt line to the outside edge of the endplate as shown in Figure 5(a). The stiffness  $K$  and prying gradient,  $Q$ , were derived to be used in an incremental solution technique. An engineer would start by determining the stiffness,  $K_{ij,k}$  and the prying gradient  $Q_{ij,k}$ . An incremental displacement  $\delta\Delta$  was generated and the incremental load  $\delta T$  and prying force  $\delta Q$  are calculated as shown below:

$$\delta T = K_{ij,k} \delta\Delta \quad (38)$$

$$\delta Q = K Q_{ij,k} \delta\Delta \quad (39)$$

Considering force equilibrium of the system, the force in the bolts,  $B$ , after pretension has been overcome can be calculated as the sum of the applied load  $T$  and the prying force  $Q$ . Moment equilibrium of the system yield the following incremental values for each displacement increment:

$$\delta B = \delta T + \delta Q \quad (40)$$

$$\delta M_{k-zone} = \delta T m - \delta Q n \quad (41)$$

$$\delta M_B = \delta Q n \quad (42)$$

The initial incremental displacement was calculated as the minimum of:

$$\delta\Delta_1 = \frac{\delta B}{K_{ij,k} + Q_{ij,k}} \quad (43)$$

$$\delta\Delta_2 = \frac{\delta M_{k-zone}}{K_{ij,k} m + Q_{ij,k} n} \quad (44)$$

$$\delta\Delta_3 = \frac{\delta M_B}{Q_{ij,k} n} \quad (45)$$

When the prying is negative, the possibility of the endplate separating completely from the column flange must also be checked and the respective deformation of the flange is calculated as follows:

$$\delta\Delta = \frac{-Q}{Q_{ij,k}} \quad (46)$$

Once the incremental forces and moments were calculated,  $M_{k-zone}$ ,  $M_B$  and  $B$  were updated, compared to their corresponding limits, the stiffness and prying gradient were updated according to the new endplate state. At the *lower bolts* level, where full separation occurs the total bolt tensile force is calculated as  $T' = \gamma\xi B$ , and added to the *upper bolts* force,  $T$ , at every incremental step. The moment limits are simply the plastic moment at the K-zone  $M_{pK-zone}$  and the bolt line  $M_{pB}$ :

$$M_{pK-zone} = \frac{F_y p t_p^2}{4} \quad (47)$$

$$M_{pB} = \left(1 - \frac{d_h}{p}\right) \frac{F_y p t_p^2}{4} \quad (48)$$

The incremental process is applied in an iterative process. Figures 9(a) and 9(b) show a comparison of the proposed endplate stiffness model versus FE results for extended endplate connections having circular bolt configuration associated with W30x108 and W 24x76 beams (where  $t_p=2.5$  cm). The proposed stiffness model predicts with excellent agreement the initial stiffness, onset of yielding, strength and deformation when compared with the FE results.

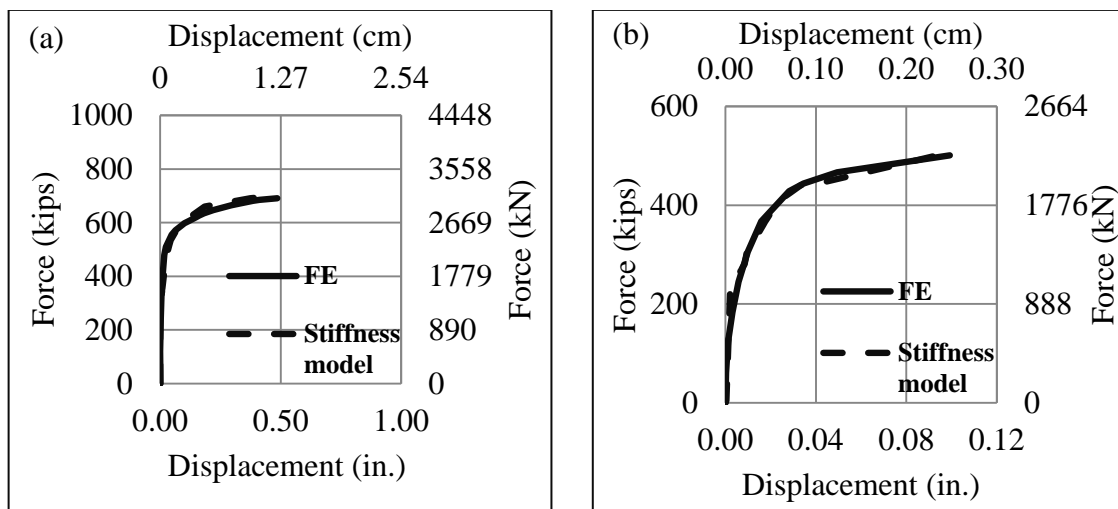


**Figure. 9.** Comparison of the FE results with the proposed extended endplate with circular bolt configuration stiffness model associated with (a) W30x108 and (b) W24x76 beams

## ***2. Column Flange with Circular Bolt Configuration***

A stiffness model was developed to predict the response of the column flange having circular bolt configuration. As discussed earlier, the bolts were divided into three *Sets* (Figure 1(c)). The proposed stiffness model, of each bolt strip, consists of two bolts characterized by a spring and a beam element for the column flange in the transversal direction as shown in Figure 5(a). The total response of the column flange is obtained by assembling the contribution from each *Set* at common incremental loads. The force and displacement were calculated according to the iterative procedure discussed in the section 10.2.1, where  $t_{cf}$  (cm) is equal to the column flange thickness ( $t_{cf}$  is considered instead of  $t_p$ ),  $m$  (cm) the length the column flange measured from the inside edge of the bolt line to the location of the K-zone and  $n$  (cm), the length of the column flange measured from the inside edge of the bolt line to the point where contact occurs between the column flange and the endplate. The tributary width per bolt,  $p$ , was calculated as per Eqn 9.

A linear interpolation is used to make sure that all the points from every *Set's* stiffness model are included in the total column flange force-deformation curve. A comparison of the force-deformation curve obtained from the proposed model and FE results for column flange having  $t_{cf} = 3.2$  cm (1.25 in.) with circular bolt configuration is shown in Figure 10. The proposed stiffness model predicts the force deformation response of the column flange with excellent agreement when compared with FE results.



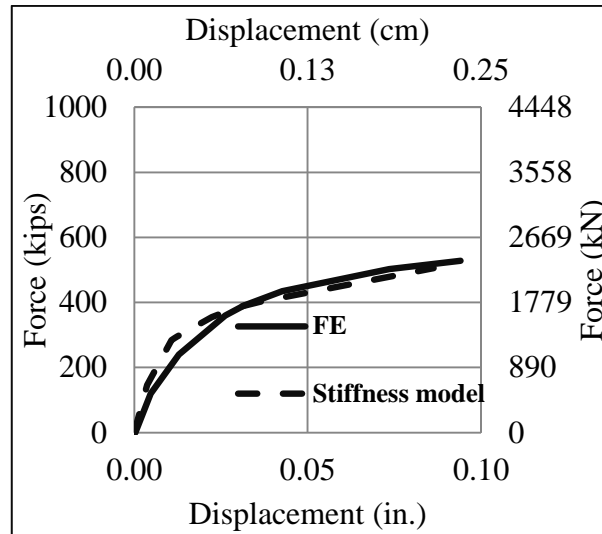


**Figure. 10.** Column flange stiffness model having circular bolt configuration associated with W30x108 beam connected to a W14x159 column ( $t_{cf}=3.2$  cm)

### C. Extended Endplate/Column System with Rectangular Bolt Configuration

#### 1. Extended Endplate with Rectangular Bolt Configuration

The extended endplate full response is modeled analytically on the basis of a beam representation for the endplate, a multi-linear spring for the bolts, accounting for the contact phenomenon (primary prying) that occurs between the endplate and the column flange assumed rigid and the beam web stiffening effect as shown in Figure 5(b). The primary prying force at the tip of the plate was simulated using pin supports.

According to the detailed FE modeling performed as part of this study, at failure, plastification of the extended endplate occurred at the K-zone followed by interior bolt fracture at the level of the *upper bolts* (Figure 1(b));. Whereas, at the *lower bolts* level, the beam web stiffens the endplate which separates from the column flange (Figure 6). Hence the *lower bolts* are subject to pure tensile force. Figure 8(b) shows the decision tree of the possible endplate limit states considered in this study. The system is

loaded by applying a vertical force  $T$  at point A (K-zone) as shown in Figure 5(b). The change of the reaction load at point C at every load increment is the prying gradient  $\Delta Q$ , and the reaction load at failure of the bolts is the primary prying force  $Q$ . The ratio of the applied force,  $T$ , at point A (K-zone) to the displacement,  $\Delta$ , of point A (K-zone) is the stiffness  $K$  of the endplate. The subscript used in the stiffness term reflects the plate limit state at the K-zone and *upper bolts* line, and the limit state of the *upper bolts*.

For instance  $K_{ee,kk}$  (Figure 8(b)), represents the stiffness of the endplate when it is in the elastic range, and the *upper bolts* are in their  $k^{\text{th}}$  stiffness range. Whereas the term  $K_{pee,kk}$ , represents the stiffness of the endplate when plastification occurred at the K-zone and the *upper bolts* are in their  $k^{\text{th}}$  stiffness step. The procedure was applied in an incremental computer automated iterative solution to simulate the mechanical response for mixed mode failure of the *upper bolts*. The change in the interior and the exterior *upper bolts* force  $\Delta B_{int}$  and  $\Delta B_{ext}$ , the change in the moment at the K-zone,  $\Delta M_{K-zone}$  and the prying gradient,  $\Delta Q$ , were generated within the software for different endplate limit states:

(1) Elastic limit state:

$$\Delta Q = \frac{\Delta T}{\left( \frac{a^3 \gamma_1}{6EI} - \frac{a(a+b+c)^2 \gamma_1}{2EI} + \frac{\gamma_1 \gamma_2 ac^2}{2EI \gamma_3} - \frac{f_s a \gamma_1}{GA} + \frac{\gamma_2}{\gamma_3} - 1 \right)} \quad (49)$$

$$\Delta B_{int} = \frac{\Delta Q \gamma_2}{\gamma_3} \quad (50)$$

$$\Delta B_{ext} = \left( \frac{\Delta Q a^3}{6EI} - \frac{\Delta Q a (a+b+c)^2}{2EI} + \frac{\Delta B_{int} ac^2}{2EI} - \frac{f_s \Delta Q a}{GA} \right) \gamma_1 \quad (51)$$

$$\Delta M_{K-zone} = \Delta T (b+c) - \Delta B_{int} b - \Delta Q a \quad (52)$$

$$K_{eee,kk} = \frac{1}{\gamma_7} \quad (53)$$

$$\gamma_1 = \frac{1}{\left( \frac{1}{K_{b1,k}} - \frac{a(b+c)^2}{2EI} \right)} \quad (54)$$

$$\gamma_2 = \frac{(a+b)^3}{6EI} - \frac{a^3 b^3 \gamma_1}{36(EI)^2} + \frac{ab^3(a+b+c)^2 \gamma_1}{12(EI)^2} + \frac{ab^3 f_s \gamma_1}{6EIGA} - \frac{(a+b)(a+b+c)^2}{2EI} + \frac{a^3(a+b)(b+c)^2 \gamma_1}{12(EI)^2} - \frac{a(a+b)(b+c)^2(a+b+c)^2 \gamma_1}{4(EI)^2} + \gamma_4 \quad (55)$$

$$\gamma_3 = \left( \frac{1}{K_{b2,k}} + \frac{ab^3 c^2 \gamma_1}{12(EI)^2} - \frac{(a+b)c^2}{2EI} - \frac{ac^2(a+b)(b+c)^2 \gamma_1}{4(EI)^2} - \frac{abc^2 f_s \gamma_1}{2GAEI} \right) \quad (56)$$

$$\gamma_4 = -\frac{a(a+b)(b+c)^2 f_s \gamma_1}{2GAEI} - \frac{(a+b)f_s}{GA} + \frac{a^3 b f_s \gamma_1}{6EIGA} - \frac{ab(a+b+c)^2 f_s \gamma_1}{2GAEI} - \left( \frac{f_s}{GA} \right)^2 ab \gamma_1 \quad (57)$$

$$\gamma_5 = \frac{a^3 \gamma_1}{6EI} - \frac{a(a+b+c)^2 \gamma_1}{2EI} + \frac{\gamma_1 \gamma_2 ac^2}{2EI \gamma_3} - \frac{f_s a \gamma_1}{GA} + \frac{\gamma_2}{\gamma_3} - 1 \quad (58)$$

$$\gamma_6 = \frac{a^3}{6EI \gamma_5} - \frac{a(a+b+c)^2}{2EI \gamma_5} + \frac{\gamma_2 ac^2}{2EI \gamma_3 \gamma_5} - \frac{f_s a}{GA \gamma_5} \quad (59)$$

$$\gamma_7 = \left[ \frac{(a+b+c)^3}{6\gamma_4} - \frac{\gamma_1 \gamma_6 (b+c)^3}{6} - \left( \frac{\gamma_2 c^3}{6\gamma_3 \gamma_4} \right) + \gamma_8 \right] \left( \frac{1}{EI} \right) + \gamma_9 \quad (60)$$

$$\gamma_8 = \left( \frac{f_s}{GA} \right) \left( - \left( \frac{a+b+c}{\gamma_4} \right) + \gamma_1 \gamma_6 (b+c) + \left( \frac{\gamma_2 c}{\gamma_3 \gamma_4} \right) \right) \quad (61)$$

$$\gamma_9 = \left( \left( \frac{-(a+b+c)^2}{2\gamma_4} \right) + \frac{\gamma_1 \gamma_6 (b+c)^2}{2} + \left( \frac{c^2 \gamma_2}{2\gamma_3 \gamma_4} \right) \right) (a+b+c) \quad (62)$$

(2) Plastic hinge formation at K-zone of plate limit state:

$$\Delta Q = \Delta T \left( 1 - \frac{b+c}{bK_{b2,k} \gamma_{10}} - \frac{b+c}{b} \right) \left( \frac{1}{\gamma_{11}} \right) \quad (63)$$

$$\Delta B_{int} = \frac{\Delta T (b+c)}{b} - \frac{\Delta Q a}{b} \quad (64)$$

$$\Delta B_{ext} = \left( \frac{\Delta B_{int}}{K_{b2,k}} - \frac{\Delta Q (a+b)^3}{6EI} - \frac{\Delta Q f_s (a+b)}{GA} + \frac{\Delta Q a^2 (a+b)}{6EI} + \frac{\Delta Q f_s (a+b)}{GA} \right) \left( \frac{1}{\gamma_{10}} \right) \quad (65)$$

$$K_{pe,kk} = \frac{1}{\gamma_{14}} \quad (66)$$

$$\gamma_{10} = \left( \frac{a+b}{aK_{b1,k}} - \frac{b^3}{6EI} + \frac{f_s b}{GA} \right) \quad (67)$$

$$\gamma_{11} = \left( \frac{-a}{bK_{b2,k}\gamma_{10}} - \frac{(a+b)^3}{6EI\gamma_{10}} + \frac{a^2(a+b)}{6EI\gamma_{10}} - 2 \right) \quad (68)$$

$$\gamma_{12} = \left( 1 - \frac{b+c}{bK_{b,2k}\gamma_{10}} - \frac{b+c}{b} \right) \left( \frac{1}{\gamma_{11}} \right) \quad (69)$$

$$\gamma_{13} = \frac{b+c-a\gamma_{12}}{K_{b,2k}} - \frac{(a+b)^3}{6EI} \gamma_{12} - \frac{f_s(a+b)\gamma_{12}}{GA} + \frac{a^2(a+b)\gamma_{12}}{6EI} + \frac{f_s(a+b)\gamma_{12}}{GA} \quad (70)$$

$$\gamma_{14} = \frac{(a+b+c)^3}{6EI} \gamma_{12} - \frac{(b+c)^3}{6EI\gamma_{10}} \gamma_{13} - \left( \frac{c^3}{6EI} \right) \left( \frac{b+c-a\gamma_{12}}{b} \right) + \gamma_{15} + \gamma_{16} \quad (71)$$

$$\gamma_{15} = \left( \frac{f_s}{GA} \right) \left( (a+b+c)\gamma_{12} + (b+c) \left( \frac{\gamma_{13}}{\gamma_{10}} \right) + \left( \frac{b+c-a\gamma_{12}}{b} \right) c \right) \quad (72)$$

$$\gamma_{16} = \left( \left( \frac{1}{K_{b1,k}a} \right) \left( \frac{\gamma_{13}}{\gamma_{10}} \right) - \frac{a^2\gamma_{12}}{6EI} + \frac{f_s\gamma_{12}}{GA} \right) (a+b+c) \quad (73)$$

Where  $\Delta T$  (kN) is the change in the applied load,  $a$  (cm) is the length of the plate measured from the inside edge of the interior bolt to the location of occurrence of the plastic hinge at the K-zone of the column flange,  $b$  (cm) is the gage distance between the tension bolts,  $c$  (cm) is the length of the plate measured from the inside

edge of the exterior bolt line to the outside edge of the extended endplate,  $\gamma_1, \gamma_2, \gamma_3, \gamma_4, \gamma_5, \gamma_6, \gamma_7, \gamma_8, \gamma_9, \gamma_{10}, \gamma_{11}, \gamma_{12}, \gamma_{13}, \gamma_{14}, \gamma_{15}$  and  $\gamma_{16}$  are constants used in the calculation of the endplate stiffness,  $A$  ( $\text{cm}^2$ ) is the cross sectional area,  $f_s$  is the shape factor used in computing the shear deformations,  $K_{b1,k}$  (kN/cm) represents the stiffness of the interior bolt in the  $k^{\text{th}}$  step, and  $K_{b2,k}$  (kN/cm) represents the stiffness of the exterior bolt in the  $k^{\text{th}}$  step.

The stiffness terms were derived to be applied in an incremental computer automated iterative solution. At the beginning the elastic stiffness of the flange  $K_{ee,11}$  is calculated from structural analysis methods. Next, several checks need to be made to determine which limit state will be reached first. The possible limit states are: (1) full plastification of the K-zone, (2) yielding of the interior bolt. Then, the prying gradient, the moment at the K-zone and the forces in the interior and exterior bolts corresponding to the current load step are computed. Finally, incremental displacement corresponding to the current load step is calculated, and the new stiffness is determined and the process is repeated again until the interior bolt force reaches  $B_{fracture}$ . After obtaining the load response for mixed mode failure of the *upper bolts* strength model, the bolt tensile force  $T'$  exhibited at the *lower bolts* level, was added to the total load at every step. At every incremental deformation  $\Delta$  (cm), the bolt force is calculated as  $B = K_{b,k}(\Delta)$ , where  $K_{b,k}$  is the corresponding bolt stiffness and  $T' = \gamma_b \xi B / 8$ .

Figures 11(a) and 11 (b) show a comparison of the proposed stiffness model versus the FE results for endplate connection associated with W30x108 and W24x76 beams. The proposed stiffness model predicts with excellent agreement the initial stiffness, onset of yielding, strength and deformation when compared with the FE results.

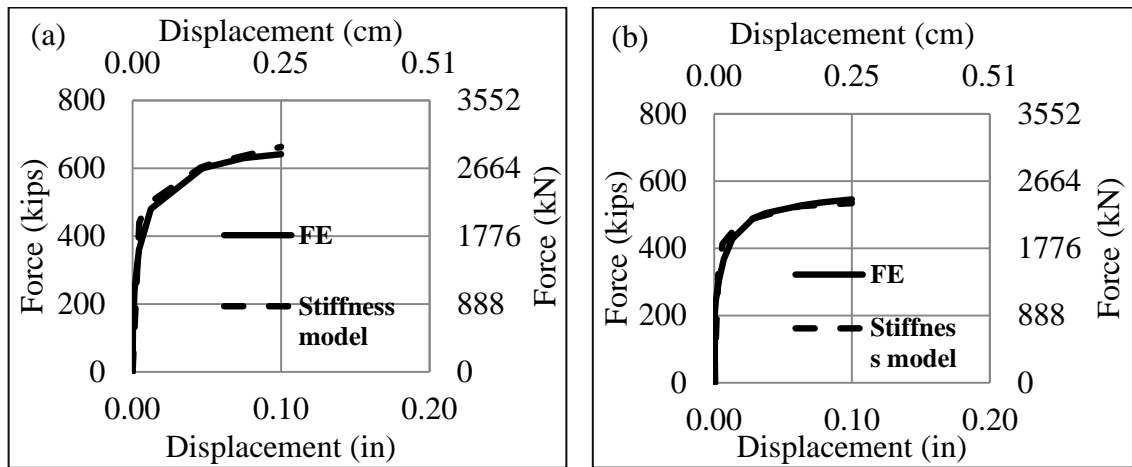


**Figure. 11.** Comparison of the FE results with the proposed extended endplate with rectangular bolt configuration stiffness model associated with (a) W 30x108 beam and (b) W24x76 beam

## 2. Column Flange with Rectangular Bolt Configuration

From the FE results, full plastification occurs at the level of the column flange with rectangular bolt configuration when  $t_{cf}$  varies between 1.9 cm (0.75 in.) and 3.2 cm (1.2 in.). The column flange was subdivided into strips consisting of two tension bolts modeled as shown in Figure 5(a). Plastic hinge will develop at the k-zone followed by the plastification of the bolt lines. The same iterative process described in section 10.2.1 is applied to get the total response of the column flange, where  $T'=T$ .

Figures 12(a), 12(b) and 12(c) show a comparison of the proposed column flange stiffness model versus the FE results for endplate/column system associated with W30x108 girders having a column flange thickness  $t_{cf}$  equal to 1.9 , 2.2 and 2.5 cm, respectively. The proposed stiffness model predicts with excellent agreement the initial

stiffness, onset of yielding, strength and deformation when compared with the FE results.

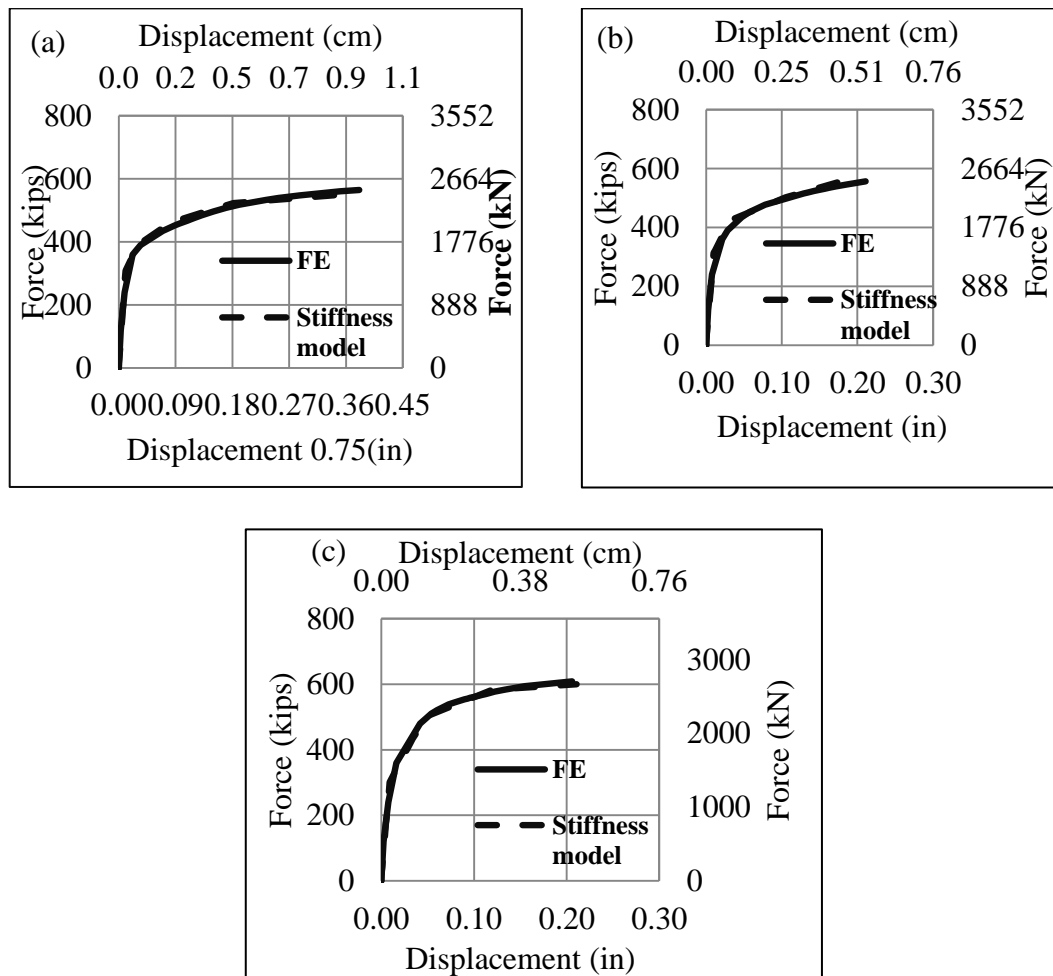


**Figure. 12.** Comparison of the FE results with the proposed column flange with rectangular bolt configuration stiffness model associated with W30x108 beam having: (a)  $t_{cf} = 1.9$  cm, (b)  $t_{cf} = 2.2$  cm and (c)  $t_{cf} = 2.5$  cm

## CHAPTER VIII

### TOTAL ASSEMBLY

After each of the different deformation mechanisms for the extended endplate and the column flange has been computed, the total force force-deformation curve of the connection is obtained by assembling the contribution from individual components at common incremental loads. Linear interpolation is used to make sure that all the load points from all the component stiffness models are included in the total force-deformation curve. Figure 13 shows a comparison of the total force-deformation curve obtained from the stiffness model and FE results for (a) extended endplate connection with circular bolt configuration associated to W24x76 beam connected to a W14x159 column, and (b) extended endplate connection with rectangular bolt configuration associated to W30x108 beam connected to a W14x82. The proposed stiffness model predicts the force-deformation response of the extended endplate/column flange system with excellent agreement when compared to the FE results.



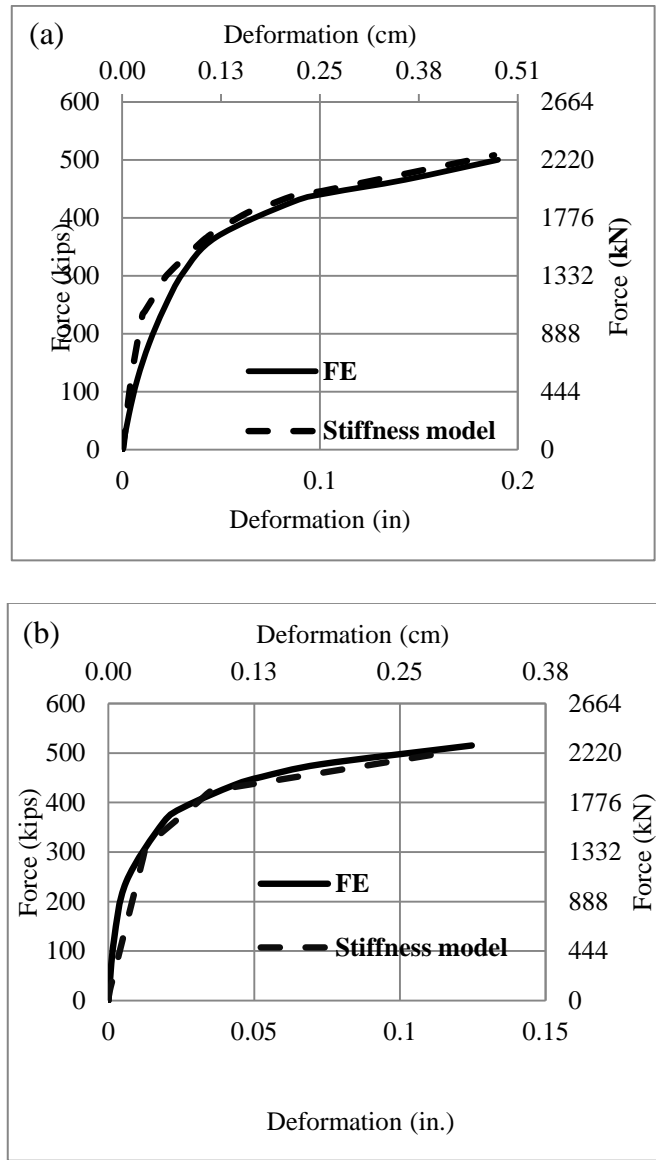


**Figure. 13.** (a) Total extended endplate connection with circular bolt configuration deformation associated with W24x76 beam including column flange deformation,(b) Total endplate connection with rectangular bolt configuration deformation associated with W30x108 beam including column flange deformation

## CHAPTER IX

### SUMMARY AND CONCLUSIONS

When designing extended endplate connections associated with deep girders, it is necessary to identify and analyze all the yielding mechanisms and failure modes. In this research, a detailed design procedure is proposed for extended endplate with circular bolt configuration associated with deep girders. A 3D nonlinear FE model was developed. A parametric study was conducted on 32 connections to investigate the effect of the circular bolt configuration on the prying phenomenon and bolt-force distribution. The prying force was quantified and analyzed based on FE results, validated with experimental results available in the literature. Extended endplate with circular bolt configuration exhibited larger prying forces when compared to its rectangular counterpart. Adopting a circular bolt configuration provides more overall ductile behavior. Strength and stiffness models that predict the deformation and capacity of the extended endplate/column flange system with circular and rectangular bolt configurations were developed. The proposed models show excellent agreement when comparing with FE and experimental results. Yield line theory was used to quantify the minimum column flange thickness requirement for the column with circular bolts pattern. One of the main advantages of the proposed models is that, in addition to its accuracy, it requires much less computational effort than that required using FE analysis, and can be used as well in more advanced modeling applications for seismic analysis and design. This study provides engineers guidelines to design extended endplate connections with circular bolt configuration.

## BIBLIOGRAPHY

ANSI/AISC Committee 358 (2010). “Prequalified Connections for Special and Intermediate Steel Moment Frames for Seismic Applications”. AISC 358-10., Chicago, Illinois, American Institute of Steel Construction.

ANSI/AISC Committee 360 (2010). “Specification for Structural Steel Buildings”. AISC 360-10., Chicago, Illinois, American Institute of Steel Construction.

Bursi, O.S & Jaspart, J.P. (2002). Calibration of a finite element model for isolated bolted end-plate steel connections. *Journal of Constructional Steel Research*, 44(3), 225-262.

Coelho, A.M.G., Bijlaard, F.S. & da Silva, L.S. (2004). Experimental assessment of the ductility of extended end plate connections, *Engineering Structures*, 26(9), 1185-1206.

Comité Européenne de Normalisation CEN, (Ed.). (2005). *EN 1993-1-1: Eurocode 3: Design of Steel Structures. Part 1-1: General Rules and Rules for Buildings*, Brussels.

Douty, R.T. & McGuire, W. (1965). High strength bolted moment connections, *Journal of the structural Division*, 91(2), 101-128.

Faella, C., Piluso, V. & Rizzano, G. (1997). A new method to design extended end plate connections and semirigid braced frames, *Journal of Constructional Steel Research*, 41(1), 61-91.

Fisher, J.W. & Struik, J.H.A. (1974). *Guide to Design Criteria for Bolted and Riveted Joints*. New York: John Wiley and Sons.

Hantouche, E.G., Kukreti, A.R. & Rassati, G.A. (2011). Investigation of secondary prying in thick built-up T-stub connections using nonlinear finite element modeling, *Engineering Structures*, 36, 113-122.

Hantouche, E.G., Kukreti, A.R., Rassati, G.A. & Swanson, J.A. (2013). Modified stiffness model for thick flange in built-up T-stub connections, *Journal of Constructional Steel Research*, 81, 76-85.

Hantouche, E.G., Kukreti, A.R., Rassati, G.A. & Swanson, J.A. (2014). “Prying Models for Strength in Thick-Flange Built-Up T-Stubs with Complete Joint Penetration and Fillet Welds, *Journal of Structural Engineering*, 141(2), 04014102.

Jaspart, J.P. & Maquoi, R. (1991). Plastic capacity of end-plate and flange cleated connections-prediction and design rules, Second international workshop on connections in steel structures: Behaviour, strength and Design, 343-352.

Kiamanesh, R., Abolmaali, A. & Razavi, M. (2012). Effect of Circular Bolt Pattern on Behavior of Extended End-Plate Connection, *Journal of Structural Engineering*, 139(11), 1833-1841.

Krishnamurthy, N. (1979). Experimental Validation of End-Plate Connection Design, Report Submitted to the American Institute of Steel Construction.

Kukreti, A.R., Murray, T.M. & Abolmaali, A. (1987). End-plate connection moment-rotation relationship, *Journal of Constructional Steel Research*, 8, 137-157.

Kulak, G.L., Fisher, J.W. & Struik, J.H.A. (1987). *Guide to Design Criteria for Bolted and Riveted Joints*. (2nd Ed.). New York: John Wiley and Sons.

Murray, T. M. (1988). Recent Developments for the Design of Moment End-Plate Connections, *Journal of Constructional Steel Research*, 10, 133-162.

Murray, T. M., & Sumner E.A. (2003) Steel Design Guide 4: Extended End-Plate Connections Seismic and Wind Applications, *American Institute of Steel Construction*, Chicago IL.

Piluso, V., Faella, C. & Rizzano, G. (2001). Ultimate behavior of bolted T-stubs. II: Model validation, *Journal of Structural Engineering*, 127(6), 694-704.

Schweizer, D.Q. (2013). *Experimental Investigation of Innovative Seismic Performance Enhancement Techniques for Steel Building Beam to Column Moment Connections* (Doctoral Thesis, North Carolina State University, Raleigh, North Carolina).

Sumner, E.A. & Murray, T.M. (2002). Behavior of extended end-plate moment connections subject to cyclic loading, *Journal of Structural Engineering*, 128(4), 501-508.

Swanson, J.A. (1999). *Characterization of the Strength, Stiffness and ductility behavior of T-Stub Connections* (Doctoral Thesis, Georgia Institute of technology, Georgia, Atlanta).

Swanson, J.A. (2002). Ultimate strength prying models for bolted T-stub connections, *Engineering Journal*, 39(3), 136-147.

Tarpy, T.S. & Cardinal, J.W. (1981). Behavior of semi-rigid beam-to-column end plate connections, *Joints in Structural Steelwork*, 2-3.